DESY 07-124
September 2007

Towards $B \to V\gamma$ Decays at NNLO in SCET

Ahmed Ali[1], **Ben D. Pecjak**[2]

Theory Group, Deutsches Elektronen-Synchrotron DESY, D-22603 Hamburg, Germany.

Christoph Greub[3]

Institute for Theoretical Physics, Univ. Berne, CH-3012 Berne, Switzerland.

April 18, 2008

Abstract

We compute NNLO ($\mathcal{O}(\alpha_s^2)$) corrections to the hard-scattering kernels entering the QCD factorization formula for $B \to V\gamma$ decays, where V is a light vector meson. We give complete NNLO results for the dipole operators Q_7 and Q_8, and partial results for Q_1 valid in the large-β_0 limit and neglecting the NNLO correction from hard spectator scattering. Large perturbative logarithms in the hard-scattering kernels are identified and resummed using soft-collinear effective theory. We use our results to estimate the branching fractions for $B \to K^*\gamma$ and $B_s \to \phi\gamma$ decays at NNLO and compare them with the current experimental data.

[1]E-mail: ahmed.ali@desy.de
[2]E-mail: pecjak@mail.desy.de
[3]Email: greub@itp.unibe.ch

1 Introduction

Radiative $B \to V\gamma$ decays, where V is a light vector meson, are processes of particular interest in flavor physics which are already accessible at the B-meson factories at SLAC and KEK; current measurements [1–7] yield the branching fractions presented in Table 1. These decays provide independent constraints on the shape of the unitarity triangle, determining the side R_t of this triangle through the ratio of branching fractions for $B \to (\rho,\omega)\gamma$ and $B \to K^*\gamma$ decays. This information is complementary to the constraints on the ratio of CKM matrix elements $|V_{td}/V_{ts}|$ obtained from the recent CDF measurement of the mass difference ΔM_s in the $B_s - \bar{B}_s$ system [8] and the already precise knowledge of the $B_d - \bar{B}_d$ mass difference ΔM_d [7]. Moreover, measurements of the CP-asymmetries in $B \to (\rho,\omega)\gamma$ decays and the isospin-violating ratio of the charged and neutral $B \to \rho\gamma$ modes would determine the inner angle α of the unitarity triangle.

The calculation of the branching fractions for $B \to V\gamma$ decays requires the evaluation of the hadronic matrix elements of the operators in the effective weak Hamiltonian. For $B \to V\gamma$ decays the weak Hamiltonian is [9, 10]:

$$\mathcal{H}_{\rm eff} = \frac{G_F}{\sqrt{2}} \sum_{p=u,c} \lambda_p^{(q)} \left[C_1 Q_1^p + C_2 Q_2^p + \sum_{i=3}^{8} C_i Q_i \right], \tag{1}$$

where $\lambda_p^{(q)} = V_{pq}^* V_{pb}$ (unitarity of the CKM matrix implies that $\lambda_t^{(q)} = -(\lambda_u^{(q)} + \lambda_c^{(q)})$ and so contributions from diagrams with top-quark loops are included implicitly). The relevant four-quark operators Q_1 and Q_2 are

$$Q_1^p = (\bar{q}\, p)_{V-A}\, (\bar{p}\, b)_{V-A}, \qquad Q_2^p = (\bar{q}_i p_j)_{V-A}\, (\bar{p}_j b_i)_{V-A}, \tag{2}$$

and the electromagnetic and chromomagnetic penguin operators Q_7 and Q_8 are

$$Q_7 = -\frac{e\,\overline{m}_b(\mu)}{8\pi^2}\, \bar{q}\, \sigma^{\mu\nu}\, [1+\gamma_5]\, b F_{\mu\nu}\,, \qquad Q_8 = -\frac{g\,\overline{m}_b(\mu)}{8\pi^2}\, \bar{q}\, \sigma^{\mu\nu}\, [1+\gamma_5]\, T^a\, b G^a_{\mu\nu}. \tag{3}$$

Here $q = d$ or s, and the convention for the sign of the couplings corresponds to the covariant derivative $iD_\mu = i\partial_\mu + eQ_f A_\mu + gT^a A^a_\mu$, with A_μ and A^a_μ representing the photon and gluon fields respectively, and $Q_e = -1$ etc. The factor $\overline{m}_b(\mu)$ is the $\overline{\rm MS}$ mass of the b quark. The Wilson coefficients C_i have been known within the next-to-leading logarithmic approximation (NLL) for over a decade (for a review, see [11]), and have been recently calculated at next-to-next-to-leading logarithmic order (NNLL) in a series of papers [12–16]. In the present work we focus on the most phenomenologically relevant operators, which are Q_1, Q_7, and Q_8. The matrix elements of the QCD-penguin operators $Q_3, \ldots Q_6$ first contribute at $\mathcal{O}(\alpha_s)$ and are multiplied by small Wilson coefficients in the weak Hamiltonian $\mathcal{H}_{\rm eff}$ (1). The contribution from Q_2 starts at $\mathcal{O}(\alpha_s^2)$.

It has been shown that in the heavy-quark limit a factorization framework (called QCD factorization) can be applied to $B \to V\gamma$ decays [17–23] (see [24,25] for phenomenological updates to NLO, and [26, 27] for the alternative "perturbative QCD" approach). In particular, the matrix element of a given operator in the effective weak Hamiltonian can be written in the form

$$\left\langle V\gamma \left| Q_i \right| \bar{B} \right\rangle = F^{B\to V_\perp}\, T_i^{\rm I} + \int d\omega\, du\, \phi_+^B(\omega)\, \phi_\perp^V(u)\, T_i^{\rm II}(\omega,u)\,. \tag{4}$$

Table 1: Status of the B-meson radiative branching fractions (in units of 10^{-6}) from the BABAR, BELLE and CLEO collaborations and their averages by HFAG [7]. The entry for $B_s \to \phi\gamma$ is from the recent BELLE measurement [6].

Mode	BABAR	BELLE	CLEO	HFAG
$B^+ \to K^{*+}\gamma$	$38.7 \pm 2.8 \pm 2.6$	$42.5 \pm 3.1 \pm 2.4$	$37.6^{+8.9}_{-8.3} \pm 2.8$	40.3 ± 2.6
$B^0 \to K^{*0}\gamma$	$39.2 \pm 2.0 \pm 2.4$	$40.1 \pm 2.1 \pm 1.7$	$45.5^{+7.2}_{-6.8} \pm 3.4$	40.1 ± 2.0
$B^+ \to \rho^+\gamma$	$1.10^{+0.37}_{-0.33} \pm 0.09$	$0.55^{+0.42+0.09}_{-0.36-0.08}$	< 13	$0.88^{+0.28}_{-0.26}$
$B^0 \to \rho^0\gamma$	$0.79^{+0.22}_{-0.20} \pm 0.06$	$1.25^{+0.37+0.07}_{-0.33-0.06}$	< 17	$0.93^{+0.19}_{-0.18}$
$B^0 \to \omega\gamma$	$0.40^{+0.24}_{-0.20} \pm 0.05$	$0.56^{+0.34+0.05}_{-0.27-0.10}$	< 9.2	$0.46^{+0.20}_{-0.17}$
$B \to K^*\gamma$	40.4 ± 2.5	42.8 ± 2.4	43.3 ± 6.2	41.8 ± 1.7
$B \to (\rho,\omega)\gamma$	$1.25 \pm 0.25 \pm 0.09$	$1.32^{+0.34+0.10}_{-0.31-0.09}$	< 14	$1.28^{+0.31}_{-0.29}$
$B_s \to \phi\,\gamma$		57^{+18+12}_{-15-17}		

The non-perturbative effects are contained in $F^{B\to V_\perp}$, the $B \to V$ transition form factor at $q^2 = 0$, and in ϕ_+^B and $\phi_\perp^V$, the leading-twist light-cone distribution amplitudes (LCDAs) of the B- and V-mesons. The hard-scattering kernels $T_i^{\rm I}$ and $T_i^{\rm II}$ include only short-distance effects and are calculable in perturbation theory. Contributions to the kernel $T^{\rm I}$ are closely related to the virtual corrections to the inclusive decay rate, and are referred to as vertex corrections. Those to the kernel $T^{\rm II}$ are related to parton exchange with the light quark in the B-meson, a mechanism commonly referred to as hard spectator scattering. It is expected that the factorization formula is valid up to corrections of $\mathcal{O}(\Lambda_{\rm QCD}/m_b)$.

The derivation of the factorization formula from a two-step matching procedure in soft-collinear effective theory (SCET) [28–31] has provided additional insight into its structure. An advantage of the effective field-theory approach is that it allows for an unambiguous separation of scales and an operator definition of each object in the factorization formula. The technical details for $B \to V\gamma$ have been provided in [32–34]. In the SCET approach the factorization formula is written as

$$\langle V\gamma\,|Q_i|\,\bar B\rangle = \Delta_i C^A \zeta_{V_\perp} + \frac{\sqrt{m_B}F\,f_{V_\perp}}{4}\int d\omega\,du\,\phi_+^B(\omega)\,\phi_\perp^V(u)\,t_i^{\rm II}(\omega,u)\,, \tag{5}$$

where F and $f_{V_\perp}$ are meson decay constants. The SCET form factor $\zeta_{V_\perp}$ is related to the QCD form factor through perturbative and power corrections [35, 37–42]. In SCET the perturbative hard-scattering kernels are the matching coefficients $\Delta_i C^A$ and $t_i^{\rm II}$. They are known completely to next-to-leading order (NLO) ($\mathcal{O}(\alpha_s)$) in renormalization-group (RG) improved perturbation theory [34]. In this paper we make steps towards a complete analysis at next-to-next-to-leading order (NNLO) by obtaining full results for the hard-scattering kernels for the dipole operators Q_7 and Q_8, and partial results for Q_1, valid in the large-β_0 limit and neglecting NNLO corrections from spectator scattering.

The hard-scattering kernels are found by matching certain partonic matrix elements in QCD with those in the effective theory. For the vertex corrections the relevant matrix elements are $\langle s\gamma|Q_i|b\rangle$. The loop corrections in the effective theory can be made to vanish by matching on-shell, so the main obstacle is the evaluation of the QCD matrix elements. However, these matrix elements are just the virtual corrections to the inclusive $B \to X_s\gamma$ decay rate. Exact results to $\mathcal{O}(\alpha_s^2)$ were obtained for Q_7 in [43, 44] and for Q_8

in [45]. For Q_1 the virtual corrections at $\mathcal{O}(\alpha_s)$ were calculated in [46–48], but those at $\mathcal{O}(\alpha_s^2)$ are known only in the large-β_0 limit [49, 50][4]. A calculation that goes beyond this approximation by employing an interpolation in the charm quark mass m_c was reported in [52], and has been used in estimating the NNLO branching fraction for the inclusive decay $B \to X_s\gamma$ [53]. However, as the calculation was not split into virtual and bremsstrahlung contributions, those results cannot be used in the SCET matching calculation. Therefore, while we obtain exact NNLO results Q_7 and Q_8, for Q_1 we are restricted to the large-β_0 limit. Our results provide an explicit check on factorization at NNLO.

Corrections from spectator scattering are included in the hard-scattering kernel $t^{\rm II}$ and first contribute to the branching fraction at NLO ($\mathcal{O}(\alpha_s)$). A complication of spectator scattering is the presence of two widely separated perturbative scales $m_b^2 \gg m_b\Lambda_{\rm QCD}$. The SCET approach provides a systematic framework for separating contributions from these two scales. In SCET the hard-scattering kernel $t_i^{\rm II}$ for a given operator is sub-factorized into the convolution of a hard-coefficient function with a universal jet function, in the form

$$t_i^{\rm II}(u,\omega) = \int_0^1 d\tau \Delta_i C^{B1}(\tau) j_\perp(\tau,u,\omega) \equiv \Delta_i C^{B1} \star j_\perp. \tag{6}$$

The hard coefficients $\Delta_i C^{B1}$ contain physics at the hard scale m_b, while the jet function $j_\perp$ contains physics at the hard-collinear scale $\sqrt{m_b\Lambda}$. The hard coefficient is identified in a first step of matching QCD $\to$ SCET$_{\rm I}$, and the jet function in a second step of matching SCET$_{\rm I}$ $\to$ SCET$_{\rm II}$. Details have been worked out for $B \to V\gamma$ in [32, 34], for heavy-to-light form factors in [36–42], and for $B \to PP$ in [54, 55].

The effective field-theory techniques are crucial for providing a field-theoretical definition of the objects in (5), and for resumming large perturbative logarithms of the ratio $m_b/\Lambda_{\rm QCD}$ in the $t_i^{\rm II}$. In the effective-theory approach resummation is carried out by solving the renormalization-group equations for the matching coefficients $\Delta_i C^{B1}$. Since these coefficients enter the factorization formula in a convolution with the jet function $j_\perp$, their anomalous dimension is a distribution in the variables τ and u. The evolution equations must be solved before performing the convolution with $j_\perp$. Therefore, resummation is not possible in the original QCD factorization formula (4), where the hard-scattering kernels $T_i^{\rm II}$ are obtained only after this convolution has been carried out.

While the SCET formalism is indispensable for resummation, in the actual matching calculations one can also use the diagrammatic method of expanding by regions [56] in order to separate hard from hard-collinear effects as in (6). This method was used to analyze loop corrections to spectator scattering for the case of the $B \to \pi$ form factor in [57], and for $B \to \pi\pi$ in [58]. In both cases the results were shown to be equivalent to those obtained directly in SCET. We use similar techniques here to compute the NNLO correction from the hard-scattering kernel $t_8^{\rm II}$. Our result for the one-loop correction at the hard-collinear scale agrees with (6), explicitly confirming the universality of the jet function predicted by SCET. Since the NNLO corrections from $t_7^{\rm II}$ are known from the form factor analysis [40, 42], the main obstacle to a complete treatment of spectator scattering is the NNLO matching calculation for Q_1.

The paper is organized as follows. In Section 2 we explain the SCET factorization framework and define the hard-scattering kernels. The SCET matching calculations are

[4]these results are obtained by calculating the $\mathcal{O}(\alpha_s^2 n_f)$ terms and then replacing $n_f \to -3\beta_0/2$, according to the hypothesis of "naive non-abelianization" [51].

carried out for the vertex corrections in Section 3 and for the hard-spectator corrections in Section 4. In Section 5 we describe the numerical analysis and estimate the branching fractions for $B \to K^\star\gamma$ and $B_s \to \phi\gamma$ decays at NNLO, comparing our results with the current data and identifying the theoretical uncertainties. We conclude in Section 6. Results for the partonic matrix elements taken from calculations for inclusive $B \to X_s\gamma$ decays are relegated to the Appendix, along with some of the SCET matching functions obtained in previous work and details of the renormalization-group analysis.

2 Factorization and the hard-scattering kernels

In this section we explain the closely related issues of factorization and extraction of the hard-scattering kernels. The objects of interest are the hadronic matrix elements

$$\left\langle V\gamma\,|Q_i|\,\bar{B}\right\rangle .$$

An analysis in [34] used a two-step matching procedure in SCET to show that these matrix elements can be written in the form (5) to all orders in perturbation theory and to leading order in $1/m_b$. In this paper we work out a large set of effective-theory matching coefficients at NNLO in perturbation theory. These are obtained by replacing the hadronic states by partonic ones and calculating the matrix elements in perturbative QCD. Showing that the partonic rate can be brought into the form (5) demonstrates factorization and provides expressions for the hard-scattering kernels.

To calculate the partonic matrix elements requires the evaluation of multi-scale Feynman integrals. It is advantageous to perform these integrals using the method of regions [56]. This not only provides a simple way to obtain results at leading order in $1/m_b$, but also a factorization of momentum scales at the level of Feynman diagrams. In this method the loop integrations are split into a sum of different regions, in which the loop momenta satisfy a fixed scaling. This allows for a Taylor expansion under the integral in each region, which is subsequently integrated over all space. The integrals are performed in dimensional regularization, where scaleless integrals are set to zero. The sum of the results for all the regions recovers the full integral, expanded in $1/m_b$.

A number of different momentum regions appear in the analysis, both perturbative and non-perturbative. To identify these we first introduce two light-like vectors $n_\pm$ satisfying $n_+n_- = 2$. We choose the outgoing vector meson to travel along the n_- direction, and define n_+ such that the velocity of the b quark is given by

$$v^\mu = n_-^\mu \frac{n_+v}{2} + n_+^\mu \frac{n_-v}{2}. \tag{7}$$

This definition implies $v_\perp = 0$, and we shall always work in the reference frame where $n_-v = n_+v = 1$. To perform the expansion in $1/m_b$, we define the parameter $\Lambda^2 = (p_B - m_bv)^2$ and the dimensionless parameter $\lambda = \Lambda/m_b \ll 1$. The regions are classified according to the scaling of their light-cone components with the expansion parameter λ. Denoting the light-cone components of a generic four-vector p by $(n_+p, p_\perp, n_-p)$, the relevant momentum regions are [34]:

Perturbative

hard	$m_b(1,1,1)$
hard-collinear	$m_b(1,\sqrt{\lambda},\lambda)$

Non-perturbative

soft	$m_b(\lambda,\lambda,\lambda)$
collinear	$m_b(1,\lambda,\lambda^2)$
soft-collinear	$m_b(\lambda,\lambda^{3/2},\lambda^2)$

The connection between the SCET analysis and perturbative QCD is provided by the method of regions. In the effective theory, contributions from the perturbative regions are encoded in Wilson coefficients of operators built from fields representing the regions of lower virtuality. It is convenient to factorize the two perturbative scales m_b^2 and $m_b\Lambda$ using a two-step matching procedure QCD $\to$ SCET$_{\rm I}$ $\to$ SCET$_{\rm II}$.

In the first matching step the hard scale m_b^2 is integrated out by matching the operators Q_i onto a set of operators in SCET$_{\rm I}$. The effective theory SCET$_{\rm I}$ involves fields for the hard-collinear and non-perturbative modes, multiplied by Wilson coefficients related to the hard region. For the case of $B\to V\gamma$, the matching takes the form [34]

$$Q_i \to \Delta_i C^A J^A + \Delta_i C^{B1} \star J^{B1} + \Delta_i C^{B2} \star J^{B2}. \tag{8}$$

The $\star$ denotes a convolution over momentum fractions, as in (6). The momentum-space Wilson coefficients depend only on quantities at the hard scale m_b^2. The exact form of the operators $J^{(i)}$ along with the relevant SCET conventions can be found in [34]:

$$J^A = \left(\bar\xi W_{hc}\right) \not\varepsilon_\perp (1-\gamma_5) h_v, \tag{9}$$

$$J^{B1} = \left(\bar\xi W_{hc}\right) \not\varepsilon_\perp \not{\mathcal{A}}_{hc_\perp} (1+\gamma_5) h_v, \tag{10}$$

$$J^{B2} = \left(\bar\xi W_{hc}\right) \not{\mathcal{A}}_{hc_\perp} \not\varepsilon_\perp (1+\gamma_5) h_v. \tag{11}$$

Here $\varepsilon_\perp$ is the polarization vector of the on-shell photon. The operators contain a hard-collinear quark field ξ, a composite object $\mathcal{A}_{hc}$, which in light-cone gauge is the hard-collinear gluon field, and W_{hc}, a Wilson line. In SCET the b-quark field is treated as in HQET. We have suppressed the arguments of the fields above, but must keep in mind that due to the non-locality of SCET the objects $\left(\bar\xi W_{hc}\right)$ and $\mathcal{A}_{hc_\perp}$ are evaluated at different points along the n_+ light-cone, whereas h_v is multipole expanded and evaluated at a point on the n_- light-cone (see, e.g., [31]). The B-type operators are actually power suppressed in SCET$_{\rm I}$, but contribute at the same order as the A-type operator upon the transition to SCET$_{\rm II}$ [36–38].

The matrix element of the operator J^A is proportional to the SCET form factor $\zeta_{V_\perp}$. The Wilson coefficients $\Delta_i C^A$ multiplying this matrix element can be extracted from calculations in the inclusive $B\to X_s\gamma$ decay. Details are given in Section 3. In contrast to the QCD form factor, the SCET form factor contains no piece which can be written in the form of a (convergent) convolution of a hard-scattering kernel with the meson LCDAs [37,38][5]. The relation between the QCD form factor and the SCET form factor

[5] although see [59] for a renewed discussion of this point.

is determined by the factorization formula [35,37,38]

$$F^{B\to V_\perp} = C^A_{V_\perp}\zeta_{V_\perp} + \frac{\sqrt{m_B}F f_{V_\perp}}{4}\int d\omega\, du\, \phi_+^B(\omega)\,\phi_\perp^V(u)\, t^{\rm II}_{V_\perp}(\omega,u)\,. \tag{12}$$

Since the matrix element of Q_7 is proportional to the form factor, the coefficient functions $C^A_{V_\perp}$ and $t^{\rm II}_{V_\perp}$ at NNLO can be determined from the results for Q_7. The exact relation is given in (80) below.

The operators $J^{(Bi)}$ can be further matched onto four-quark operators in $\mathrm{SCET_{II}}$. For $B\to V\gamma$ decays, only the operator J^{B1} is relevant. The matrix element of the four-quark operator onto which it matches factorizes into a product of LCDAs for the B and V mesons. The operator J^{B2}, on the other hand, matches onto a four-quark operator whose renormalized matrix element has no projection on the pseudoscalar B-meson LCDA. In matching the operator J^{B1} onto $\mathrm{SCET_{II}}$ the hard-collinear scale $m_b\Lambda$ is integrated out, and the associated Wilson coefficient is the jet function $j_\perp$. The final low-energy theory $\mathrm{SCET_{II}}$ contains only soft, collinear, and soft-collinear fields. Factorization means that soft fields are restricted to the B-meson LCDA, and collinear ones to the V-meson LCDA. Since these two pieces communicate only through soft-collinear interactions, factorization amounts to showing that such contributions decouple from the hadronic matrix element of the $\mathrm{SCET_{II}}$ operator. This was done in [34]. Thus the matrix element of the operator onto which J^{B1} matches is exactly of the form of the second piece of (5), with $t_i^{\rm II} = \Delta_i C^{B1}\star j_\perp$. This same jet function appears in the factorization formula (12) for the form factor, where $t^{\rm II}_{V_\perp} = C^{B1}_{V_\perp}\star j_\perp$. We can summarize this discussion by the following factorization formula

$$\begin{aligned}\langle V\gamma\,|Q_i|\,\bar B\rangle &= \Delta_i C^A\zeta_{V_\perp} + \frac{\sqrt{m_B}F f_{V_\perp}}{4}\left(\Delta C^{B1}\star j_\perp\right)\star\phi_\perp^V\star\phi_+^B \\ &= \frac{\Delta_i C^A}{C^A_{V_\perp}}F^{B\to V_\perp} + \frac{\sqrt{m_B}F f_{V_\perp}}{4}\left[\left(\Delta_i C^{B1} - \frac{\Delta_i C^A}{C^A_{V_\perp}}C^{B1}_{V_\perp}\right)\star j_\perp\right]\star\phi_\perp^V\star\phi_+^B.\end{aligned} \tag{13}$$

This formula relates the hard-scattering kernels $\Delta_i C^A$ and $t_i^{\rm II}$ in (5) to the Wilson coefficients from the two-step matching procedure in SCET, and provides a connection with the original formulation (4). For instance, using that $\Delta_7 C^i \sim C^i_{V_\perp}$, one can verify that Q_7 contributes to both terms in the SCET formulation, but only to the vertex term in the original formulation.

A main result of our paper is an expression for the $\mathcal{O}(\alpha_s^2)$ correction to the hard coefficient $\Delta_8 C^{B1}$. We obtain it with a straightforward diagrammatic analysis using the method of regions, without the explicit formulation of SCET or the use of its Feynman rules. Since contributions from J^{B1} can be uniquely identified by the Dirac structure of the four-quark operator onto which it matches, the sub-factorization of the hard-scattering kernel into a convolution of a jet and hard function can be performed by separating out the contributions of the hard and hard-collinear regions multiplying this structure. Details are given in Section 4.

3 Vertex corrections

We begin with the vertex corrections, extracting the contributions of the operators Q_1, Q_7, and Q_8 to the SCET Wilson coefficient C^A at NNLO ($\mathcal{O}(\alpha_s^2)$). To do so we calculate the

partonic matrix elements

$$\langle Q_i \rangle \equiv \langle q(p)\gamma(q)|Q_i|b(p_b)\rangle$$

to this same order in both SCET and QCD. This matrix element is chosen because it contains no external gluons and so matches directly onto the operator J^A in (9). The calculation is performed with on-shell external quark states and both UV and IR divergences are regularized dimensionally. In that case the matching calculation is simple, because the loop corrections in SCET are scaleless and vanish. The matrix element of J^A is just the tree expression plus counterterms from wave-function and current renormalization. The QCD matrix elements can be read off from the virtual corrections to the inclusive decay $B \to X_s\gamma$. Using that the on-shell wave-function renormalization factors in the effective theory are unity, and replacing the bare SCET current by its renormalized one, we have

$$\langle Q_i \rangle = D_i \langle Q_{7,\text{tree}} \rangle = \Delta_i C^A Z_J \langle J^A_{\text{tree}} \rangle. \tag{14}$$

Here the D_i are the scalar amplitudes in QCD, the $\Delta_i C^A$ are the contributions of a given operator to the SCET matching coefficient, and Z_J is the renormalization factor of the SCET current operator J_A. Each of these quantities is determined as a series in α_s. For the operators $Q_{7,8}$ we can obtain complete results at NNLO, while for Q_1 we can only provide an estimate using the large-β_0 limit.

We first consider tree level, where only Q_7 contributes. For on-shell matching the spinors in QCD and SCET are equal to one another and we find

$$\Delta_7 C^{A(0)} = -\frac{e\,\overline{m}_b\,2E_\gamma}{4\pi^2}, \tag{15}$$

where the photon energy is $2E_\gamma = m_B(1 - m_V^2/m_B^2) \approx m_b$ in the heavy-quark limit. At higher orders the matching coefficients can be read off from the functions D_i according to the relation

$$\Delta_i C^A(m_b,\mu) = \Delta_7 C^{A(0)} \lim_{\epsilon\to 0} Z_J^{-1}(\epsilon, m_b, \mu)\, D_i(\epsilon, m_b, \mu)\,. \tag{16}$$

The SCET current renormalization factor Z_J is determined by requiring that the Wilson coefficient be free of IR poles.

Before giving results for the higher-order corrections, we pause to explain a subtlety in the matching which first appears at two loops. The on-shell matrix elements of the QCD operators Q_i are calculated in $\overline{\text{MS}}$ renormalization in the five-flavor theory, $n_f = n_l + n_h$ with $n_h = 1$ for the b quark. However, in SCET b-quark loops are absent and the matrix elements are calculated as an expansion in the four-flavor theory. In order to perform a correct matching, it is necessary to express the UV renormalized results in the five-flavor theory in terms of the four-flavor parameters of SCET. A similar problem arises when integrating out the top quark to match the Standard Model onto the effective weak Hamiltonian. The solution is to renormalize the coupling constant in the $n_f = n_h + n_l$ flavor theory according to $\alpha_s^{\text{bare}} = Z_\alpha^{n_h+n_l}\alpha_s$, with (see e.g. [13, 60])

$$Z_\alpha^{n_h+n_l} = 1 - \frac{\alpha_s}{4\pi\epsilon}\left[\frac{11}{3}C_A - \frac{2}{3}n_f + \frac{2}{3}n_h(1 - N_\epsilon)\right]. \tag{17}$$

The function N_ϵ is fixed such that α_s is the $\overline{\text{MS}}$-renormalized coupling in the *four* flavor theory. Its value is

$$N(\epsilon) = e^{\gamma\,\epsilon}\left(\frac{\mu^2}{m_b^2}\right)^\epsilon \Gamma(1+\epsilon)\,. \tag{18}$$

Results for the scalar amplitudes D_i in this renormalization scheme can be obtained from the $\overline{\rm MS}$ results given in the Appendix by making the replacement

$$\alpha_s \to \alpha_s \left(1 + \frac{\alpha_s}{4\pi}\frac{4}{3} n_h \left[L + \epsilon\left(L^2 + \frac{\pi^2}{24}\right) + \epsilon^2\left(\frac{2L^3}{3} + \frac{\pi^2}{12}L - \frac{\zeta_3}{6}\right)\right]\right) + \dots\,, \tag{19}$$

where $L = \ln \mu/m_b$. Note that this is just the standard decoupling relation when evaluated in four dimensions.

We now give results for the Wilson coefficients, which we write in the form

$$\Delta_i C^A = \Delta_7 C^{A(0)} \left[\delta_{i7} + \frac{\alpha_s(\mu)}{4\pi}\Delta_i C^{A(1)} + \left(\frac{\alpha_s(\mu)}{4\pi}\right)^2 \Delta_i C^{A(2)}\right]. \tag{20}$$

We begin with Q_7. Results can be given analytically, but since those for Q_8 are only known numerically we treat Q_7 the same. Using the scalar functions D_7 given in the Appendix we find

$$\begin{aligned}
\Delta_7 C^{A(1)} &= C_F\left[-2L^2 - 5L - 2L_{\rm QCD} - 6.8225\right], \\
\Delta_7 C^{A(2)} &= C_F^2\left(2L^4 + 14L^3 + 38.1449L^2 + 56.14711L + 7.8159\right) \\
&\quad + C_F C_A\left(-4.8889L^3 - 33.9758L^2 - 92.3415L - 83.8866\right) \\
&\quad + C_F n_l\left(0.8889L^3 + 6.8889L^2 + 19.9050L + 23.8254\right) \\
&\quad + C_F n_h\left(-1.3333L^2 + 2.8889L - 0.810288\right),
\end{aligned} \tag{21}$$

where one is to use $n_l = 4$ and $n_h = 1$ in the above equation. In the one-loop result we have distinguished the logarithms $L_{\rm QCD} = \ln \mu_{\rm QCD}/m_b$ and $L = \ln \mu/m_b$. The $\mu_{\rm QCD}$ dependence cancels against the scale dependence in the effective weak Hamiltonian, whereas the μ dependence cancels against the scale dependence of the SCET soft function $\zeta_{V_\perp}$ and the running coupling constant. At one loop it is straightforward to separate the logarithms by identifying the UV and IR poles in the individual Feynman diagrams. At two loops the distinction can be made by using the renormalization-group equation (25) below. We give explicit results for the case where L is distinguished from $L_{\rm QCD}$ in the Appendix, but in this section we quote the NNLO results only for $L = L_{\rm QCD}$.

We can use our results to determine the anomalous dimension of the operator J^A up to two loops. The anomalous dimension is obtained from the coefficient $Z_J^{(1)}$ of the $1/\epsilon$ pole term in the current renormalization factor and has the form

$$\gamma^A = 2\alpha_s \frac{\partial}{\partial \alpha_s} Z_J^{(1)}(m_b, \mu) = -\Gamma_{\rm cusp}(\alpha_s)\,\ln\frac{\mu}{m_b} + \gamma^J(\alpha_s)\,, \tag{22}$$

where $\Gamma_{\rm cusp}$ is the cusp anomalous dimension appearing in the renormalization-group theory of Wilson lines [61] (it has recently been calculated to three loops [62]; the result is listed in the appendix). The result for the renormalization factor to two loops is

$$\begin{aligned}
Z_J &= 1 + \frac{C_F\alpha_s}{4\pi}\left[-\frac{1}{\epsilon^2} - \frac{5}{2\epsilon} - \frac{2L}{\epsilon}\right] \\
&+ C_F\left(\frac{\alpha_s}{4\pi}\right)^2\left[-\frac{0.5C_F}{\epsilon^4} + \frac{1}{\epsilon^3}\left(-2.5C_F + 2.75C_A - 0.5n_l - 2C_F L\right)\right. \\
&+ \frac{1}{\epsilon^2}\left(-3.125C_F + 3.5447C_A - 0.5556n_l - 2C_F L^2 + (-5C_F + 3.6667C_A - 0.6667n_l)L\right) \\
&\left.+ \frac{1}{\epsilon}\left(-2.6525C_F - 3.4386C_A + 1.9799n_l + (-4.1546C_A + 1.1111n_l)L\right)\right],
\end{aligned} \tag{23}$$

from which we find

$$\begin{aligned}\gamma^A &= \frac{C_F\alpha_s}{4\pi}(-4L-5) \\ &\quad + C_F\left(\frac{\alpha_s}{4\pi}\right)^2\left((-16.6183C_A+4.444n_l)L-10.6102C_F-13.7545C_A+7.9195n_l\right).\end{aligned} \tag{24}$$

This is consistent with (22) and defines γ^J. The one-loop result was first obtained in [29]. We note that in this case the n_h dependence in the renormalization factor Z_J drops out after using (19). This must be the case, since in the effective-theory current the b quark is integrated out and so its anomalous dimension cannot depend on n_h. Our result for the anomalous dimension, along with the relation

$$\mu\frac{d}{d\mu}\Delta_i C^A = \gamma^A \Delta_i C^A\,, \tag{25}$$

allows us to perform the separation of UV and SCET logs in the Wilson coefficients given in the Appendix.

The same SCET current also appears in the study of the inclusive $B\to X_s\gamma$ decay spectrum with a cut on the photon energy [63]. A result equivalent to our two-loop matching coefficient $\Delta_7 C^{A(2)}$ with $\mu=m_b$ was recently obtained in [64]. Translating our expression into the two-loop result for $h(1)$ given in [64], we find numerical agreement. The dependence on n_h not taken into account in that work is negligible numerically. We can also check the two-loop anomalous dimension by using RG-invariance of the inclusive decay rate along with the anomalous dimensions of the jet and soft functions calculated in [65,66]. Here again the results agree.

We repeat the calculation for Q_8. In this case the one-loop result is IR finite. The two-loop matching equation also becomes IR finite after the results are expressed in terms of the renormalized current calculated above. This is a check on the effective-theory construction, according to which the IR poles in the QCD amplitudes for each operator in the weak Hamiltonian are absorbed by the same SCET current. For the coefficient functions we find

$$\begin{aligned}\Delta_8 C^{A(1)} &= C_F\left[2.6667L_{\rm QCD}+1.4734+2.0944i\right], \\ \Delta_8 C^{A(2)} &= -C_F^2\big[5.3333L^3+32.2802L^2+50.9612L+1.8875 \\ &\quad +i(4.1888L^2+31.4159L+29.8299)\big] \\ &\quad +C_FC_A\big[15.1111L^2+31.6617L+2.3833+i(23.7365L+28.0745)\big] \\ &\quad -C_Fn_l\big[1.7778L^2+4.0386L+1.7170+i(2.7925L+4.4215)\big] \\ &\quad +C_Fn_h\big[1.7778L^2-2.0741L+0.8829\big].\end{aligned} \tag{26}$$

Finally, we consider the four-quark operators Q_1 and Q_2. At NLO the contribution from Q_1 can be obtained as an expansion in m_c^2/m_b^2, whereas that from Q_2 vanishes. To extract the NNLO results for these operators would require the QCD amplitudes D_1 and D_2 to this same order, which involves the calculation of a large set of three-loop graphs. These corrections are known exactly only in the large-β_0 limit, in an expansion in $z=m_c^2/m_b^2$ [49]. Within this approximation the result for Q_2 vanishes, and that for Q_1 can be written as

$$\begin{aligned}\Delta_1 C^{A(1)} &= \frac{m_b}{\overline{m}_b}C_F\left[-3.8519L_{\rm QCD}+r^{(1)}(z)\right], \\ \Delta_1 C^{A(2)} &= -\frac{3\beta_0}{2}\frac{m_b}{\overline{m}_b}C_F\left[2.4691L^2+l^{(2)}(z)L+r^{(2)}(z)\right],\end{aligned} \tag{27}$$

where we have replaced $n_f \to -3\beta_0/2$ as appropriate in the large-β_0 limit. Within this limit it is also consistent to set the ratio $m_b/\overline{m}_b$ to unity, as we shall do in the numerical analysis of Section 5. Since in the large-β_0 limit the amplitude is IR finite, we can read off the functions $r^{(i)}$ and $l^{(2)}$ directly from the results for inclusive $B \to X_s\gamma$ decay. Converting to our notation we have

$$r^{(1)} = \frac{r_2}{C_F}, \qquad r^{(2)} = \frac{r_2^{(2)}}{C_F} \qquad l^{(2)} \;=\; -\frac{l_2^{(2)}}{C_F}\,, \tag{28}$$

where r_2 is defined in eq. (2.35) of [46], and $r_2^{(2)}, l_2^{(2)}$ in eq. (22) of [49]. As an example, for $m_c/m_b = 1.2/4.8$ we have

$$\begin{aligned}
\Delta_1 C^{A(1)} &= \frac{m_b}{\overline{m}_b} C_F \left[-3.8519 L_{\rm QCD} - 3.4529 - 0.5138 i\right], \\
\Delta_1 C^{A(2)} &= -\frac{3\beta_0}{2}\frac{m_b}{\overline{m}_b} C_F \left[2.4691 L^2 + 4.9083 L + 5.1203 + i(0.9953 L + 1.6014)\right].
\end{aligned} \tag{29}$$

There are two major uncertainties associated the large-β_0 limit. The first is that there is no way to quantify the size of the terms in $\Delta_1 C^{A(2)}$ not captured within this limit. The second is that the higher-order calculation does not resolve the perturbative ambiguities in the ratios of quark masses $m_b/\overline{m}_b$ and m_c/m_b in the lower-order coefficient $\Delta_1 C^{A(1)}$: the difference between mass renormalization schemes in these ratios is a correction proportional to $C_F\alpha_s$ and set to zero in the large-β_0 limit. We discuss these uncertainties in more detail in the numerical analysis of Section 5.

In Section 5 we will be interested in the dependence of the branching fractions on the choice of renormalization scales. Both the matching coefficients $\Delta_i C^A$ and the SCET soft function $\zeta_{V_\perp}$ depend on the SCET factorization scale μ. It is convenient to use the renormalization group to determine the coefficients $\Delta_i C^A$ at an arbitrary scale μ, given their value at a matching scale $\mu_h \sim \mu_{\rm QCD} \sim m_b$. This allows us to fix $\mu = m_b$ and determine the soft function $\zeta_{V_\perp}$ only at this single scale. We can then study the dependence of the branching fractions under variations in μ_h and $\mu_{\rm QCD}$, under which it is formally invariant. The relevant RG formalism was worked out in [41]. The expression we need is

$$\Delta_i C^A(m_b, \mu_h, \mu) = \left(\frac{m_b}{\mu_h}\right)^{a(\mu_h,\mu)} \exp[S(\mu_h,\mu) + a_J(\mu_h,\mu)]\, \Delta_i C^A(m_b, \mu_{\rm QCD} = \mu_h, \mu_h)\,. \tag{30}$$

In the above equation we have correlated the scales $\mu_{\rm QCD} = \mu_h$ for simplicity, although we can keep them separate using the results in the Appendix. With this choice the dependence on $\mu_h = \mu_{\rm QCD}$ on the left-hand side cancels against the dependence in the effective weak Hamiltonian, so that the branching fractions are invariant under variations of the matching scale μ_h. The RG exponents S and a, and a_J are given by

$$S(\mu_1,\mu_2) \;=\; -\int_{\alpha_s(\mu_1)}^{\alpha_s(\mu_2)} \frac{d\alpha}{\beta(\alpha)} \Gamma_{\rm cusp}(\alpha) \int_{\alpha_s(\mu_1)}^{\alpha} \frac{d\alpha'}{\beta(\alpha')}, \tag{31}$$

$$a(\mu_1,\mu_2) \;=\; \int_{\alpha_s(\mu_1)}^{\alpha_s(\mu_2)} \frac{d\alpha}{\beta(\alpha)} \Gamma_{\rm cusp}(\alpha), \tag{32}$$

$$a_J(\mu_1,\mu_2) \;=\; \int_{\alpha_s(\mu_1)}^{\alpha_s(\mu_2)} \frac{d\alpha}{\beta(\alpha)} \gamma_J(\alpha). \tag{33}$$

These exact solutions are evaluated by expanding the anomalous dimensions and the QCD β-function as perturbative series in the strong coupling. We can do this to two-loop order for a and a_J, and to three-loop order for S. The expansions to this order are listed in the Appendix.

4 Hard spectator scattering

In this section we consider the spectator scattering mechanism and the calculation of $t_i^{\rm II}$ ($i = 1, 7, 8$). The leading corrections from spectator scattering contribute to the branching fractions at NLO ($\mathcal{O}(\alpha_s)$) and are known completely. The NNLO corrections from Q_7 are also known [34], since they can be taken from the heavy-to-light form factor analysis in [39, 40, 42]. In this section we calculate the NNLO corrections from Q_8. We find agreement with a certain set of logarithmic corrections obtained in [67], and verify the important SCET result that contributions at the hard-collinear scale for each operator in the effective weak Hamiltonian are taken into account by a universal jet function. To complete the NNLO matching calculation for spectator scattering would require results for Q_1 and Q_2. This is a rather difficult calculation involving the evaluation of two-loop graphs depending on the ratio m_c/m_b.

Before presenting our results for Q_8, we first review the results for Q_7 as derived in [34]. This will fix some notation and clarify the sub-factorization of $t_i^{\rm II}$ into a convolution of hard and jet functions. The calculation makes use of the two-step matching procedure outlined in Section 2 to integrate out the perturbative scales $m_b^2 \gg m_b\Lambda_{\rm QCD}$. At tree level and to leading order in the HQET expansion the result is

$$t_7^{\rm II(0)}(u,\omega) = \int_0^1 d\tau\, \Delta_7 C^{B1(0)}(\tau) j_\perp^{(0)}(\tau,u,\omega), \tag{34}$$

where

$$\Delta_7 C^{B1(0)}(\tau) = \frac{e\overline{m}_b}{4\pi^2}; \qquad j_\perp^{(0)}(\tau,u,\omega) = -\frac{4\pi C_F\alpha_s}{N_c}\frac{1}{m_b\omega\bar{u}}\delta(\tau-u)\,. \tag{35}$$

The one-loop correction to the hard-scattering kernel breaks into a sum of corrections to the hard coefficient and the jet function according to

$$t_7^{\rm II(1)} = \Delta_7 C^{B1(1)} \star j_\perp^{(0)} + \Delta_7 C^{B1(0)} \star j_\perp^{(1)}, \tag{36}$$

where the superscripts denote the (n)-loop correction to each function and the $\star$ denotes a convolution over the variable τ. Explicit results for each term can be deduced from the form-factor analysis in [39, 40, 42] and are listed in the Appendix. Note that while the hard coefficient function $\Delta_7 C^{B1}$ is particular to the operator Q_7, the jet function $j_\perp$ is not. It is determined by the matching step $\text{SCET}_I \to \text{SCET}_{\rm II}$, which contains no information about the structure of the operators in the effective weak Hamiltonian at the scale m_b. In the SCET description of spectator scattering, therefore, the non-trivial task is to determine the corrections at the hard scale m_b, contained in the Wilson coefficients $\Delta_i C^{B1}$. The contributions at the hard-collinear scale $m_b\Lambda$ can be obtained by performing the convolution in the second term of (36).

In what follows we obtain an expression for $t_8^{\rm II(1)}$ in the form (36), derived in the following way. We first calculate the hard-scattering kernel directly in QCD factorization,

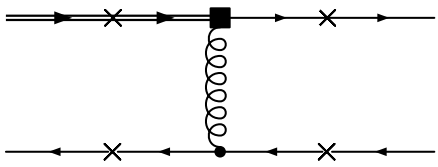

Figure 1: The lowest-order diagram for spectator scattering with Q_8. The double-line represents the incoming b quark and the solid box an insertion of Q_8. The photon can be attached to any of the four crosses. Only photon emissions from the light quark emerging from the Q_8 insertion contributes at leading power in $1/m_b$.

but separate the contributions from the hard and hard-collinear scales using the method of regions. We then show that the one-loop contribution from the hard-collinear region is exactly $\Delta_8 C^{B1(0)} \star j_\perp^{(1)}$. Since both the coefficient function $\Delta_8 C^{B1(0)} \sim \bar\tau/\tau$ (with $\bar\tau \equiv 1-\tau$) and the jet function $j_\perp^{(1)}$ are non-trivial functions of τ, this provides a consistency check between the QCD factorization and the SCET formalism, and also a check on our loop calculations. The remaining contribution is from the hard region and is identified with $\Delta_8 C^{B1(1)} \star j_\perp^{(0)}$. Since $j_\perp^{(0)}$ is a delta function in the variable τ, this result is sufficient to recover the coefficient function $\Delta_8 C^{B1(1)}$. As mentioned in the Introduction, it is this τ-dependent function which is needed to obtain the resummed hard-scattering kernel used in the numerical analysis in Section 5.

4.1 Q_8 at tree level

We start by reviewing the tree-level calculation. The strategy is to evaluate the partonic matrix element $\mathcal{A}_8 = \langle q(p_1)\,\bar q'(p_2)\gamma(q)\,|\,Q_8\,|\,\bar q'(k)\,b(p_b)\rangle$ and show that it can be written in the form (5). The hard-scattering kernel is independent of the exact choice of the partonic momenta. We shall work with on-shell quarks in the initial and final states, and furthermore work in the reference frame where the perpendicular components of the external parton momenta vanish. In this frame, the momenta can be chosen as $p_1 = up$, $p_2 = \bar u p$, $k = \omega n_+/2$, $p_b = m_b v = p_B - k$, and $q = E_\gamma n_+$, with $\bar u \equiv 1-u$. At leading order in $1/m_b$ we can write the vector-meson momentum as $p \approx m_b n_-/2$ and the photon energy as $E_\gamma \approx m_b/2$. The photon's polarization vector lies in the transverse plane and is denoted by $\epsilon_\perp$. The power counting is such that $\omega/m_b \sim \lambda \ll 1$.

The four Feynman diagrams which can contribute at tree-level are represented in Figure 1. The photon can be emitted from any of the four crosses. At leading order in λ only the diagram where the photon is attached to the light quark produced at the flavor-changing weak current contributes. Emissions from the other quark lines are either power suppressed or have no projection on the meson LCDAs. For the tree-level scattering amplitude one finds

$$\begin{aligned}\mathcal{A}_8^{(0)} &= \frac{\overline{m}_b}{m_b}\frac{eQ_d\alpha_s}{\pi}\,\frac{\bar u}{u}\frac{1}{\bar u\,\omega}\left[\bar u(up)\,\{\not\epsilon_\perp\gamma_{\nu_\perp}\,(1+\gamma_5)\}\,T^a u(p_b)\right]\left[\bar v(k)\gamma_\perp^\nu T^a v(\bar u p)\right]\\ &= \frac{\overline{m}_b}{m_b}\frac{C_F}{N_c}\frac{eQ_d\alpha_s}{\pi}\,\frac{\bar u}{u}\frac{1}{\bar u\,\omega}\,\left[\not\epsilon_\perp\gamma_{\nu_\perp}\otimes\gamma_\perp^\nu\right] \equiv A^{(0)}\,\left[\not\epsilon_\perp\gamma_{\nu_\perp}\otimes\gamma_\perp^\nu\right],\end{aligned} \tag{37}$$

where u and v represent the free-particle spinor wave-functions and $Q_d = -1/3$ denotes the charge of a down-type quark. We have distinguished the $\overline{\rm MS}$ mass $\overline{m}_b(\mu)$ from the

pole mass m_b, anticipating the one-loop calculation in the next section. To obtain the second line we already performed the color trace, so that the notation $\Gamma_1 \otimes \Gamma_2$ is to be understood as the Dirac structure between quark spinors. In the second line we defined the tree-level partonic amplitude $A^{(0)}$. At tree level there is only one Dirac structure, related to the matching of the $\mathrm{SCET_I}$ operator J^{B1}.

To proceed further we need definitions for the LCDAs in the low-energy theory $\mathrm{SCET_{II}}$. The light-cone projection operator $\Phi^H_{\alpha\beta}(\tilde{k})$ onto a heavy state H containing the b-quark is given by

$$\Phi^H_{\alpha\beta}(\tilde{\omega}) = \int \frac{dt}{2\pi}\, e^{it\tilde{\omega}} \,\langle 0\,|\bar{q}_{s\,\beta}(tn_-)\,[tn_-,0]\,h_{v\alpha}(0)|\,H(v)\rangle\ , \tag{38}$$

where q_s and h_v are soft and heavy quark fields in HQET; α and β are spinor labels. The quantity $[tn_-,0]$ denotes a path-ordered exponential along the light cone. Similarly, the light-cone projection operator $\Phi^V_{\gamma\delta}(u)$ onto a light meson state L is defined by

$$\Phi^L_{\gamma\delta}(u) = n_+p \int \frac{ds}{2\pi}\, e^{-isun_+p} \left\langle L(p)\left|\bar{\xi}_\delta(sn_+)\,[sn_+,0]\,\xi_\gamma(0)\right|0\right\rangle\ , \tag{39}$$

where the ξ are collinear quark fields in SCET. The hadronic matrix elements of these light-cone projection operators, contracted with certain Dirac structures, are the LCDAs of the B and V mesons. The exact definitions of the distribution amplitudes needed in the analysis are

$$\begin{aligned}
\langle 0|\bar{q}_s(tn_-)[tn_-,0]\frac{\not{n}_-}{2}h_v(0)|B(v)\rangle &= -\frac{iF(\mu)}{2}\sqrt{m_B}\,\mathrm{tr}\Big[\frac{\not{n}_-}{2}\frac{1+\not{v}}{2}\gamma_5\Big]\int_0^\infty d\omega e^{-i\omega t}\phi_+^B(\omega,\mu)\\
\langle V(p)|\bar{\xi}(sn_+)\,[sn_+,0]\,\gamma_\perp^\mu\frac{\not{n}_+}{2}\xi(0)|0\rangle &= \frac{if_{V_\perp}(\mu)}{4}n_+p\,\mathrm{tr}\Big[\not{\eta}_\perp\gamma_\perp^\mu\frac{\not{n}_+\not{n}_-}{4}\Big]\int_0^1 du\, e^{isun_+p}\phi_\perp^V(u,\mu),
\end{aligned} \tag{40}$$

where $\eta_\perp$ is the polarization vector of the V-meson.

To extract the hard-scattering kernels we need only the partonic matrix elements. We write these as a product of scalar distribution functions multiplied by appropriate Dirac spinors. For on-shell matching at leading order in $1/m_b$ the QCD spinors are equal to the effective theory ones. At lowest order we have

$$\Phi^{b\bar{q}'(0)}_{\alpha\beta}(\omega') = \phi^{b\bar{q}'(0)}\,\bar{v}_\beta(k)\,u_\alpha(p_B-k) = \delta(\omega-\omega')\,\bar{v}_\beta(k)\,u_\alpha(p_B-k), \tag{41}$$

$$\Phi^{q\bar{q}'(0)}_{\gamma\delta}(x) = \phi^{q\bar{q}'(0)}\,\bar{u}_\delta(up)\,v_\gamma(\bar{u}p) = \delta(u-x)\,\bar{u}_\delta(up)\,v_\gamma(\bar{u}p), \tag{42}$$

and $\mathcal{A}_8^{(0)}$ can be written in the factorized form

$$\mathcal{A}_8^{(0)} = \Phi^{b\bar{q}'(0)} \star \mathcal{T}_8^{\mathrm{II}(0)} \star \Phi^{q\bar{q}'(0)}, \tag{43}$$

with

$$\begin{aligned}
\mathcal{T}^{\mathrm{II}(0)}_{8,\,\alpha\beta\gamma\delta}(\omega,u) &= \frac{\overline{m}_b}{m_b}\frac{C_F}{N_c}\frac{eQ_d\alpha_s}{\pi}\,\frac{1}{u\omega}\,\{\not{\epsilon}_\perp\gamma_{\nu_\perp}(1+\gamma_5)\}_{\delta\alpha}\,\{\gamma^{\nu_\perp}\}_{\beta\gamma}\\
&\equiv t_8^{\mathrm{II}(0)}\,\{\not{\epsilon}_\perp\gamma_{\nu_\perp}(1+\gamma_5)\}_{\delta\alpha}\,\{\gamma^{\nu_\perp}\}_{\beta\gamma}\,.
\end{aligned} \tag{44}$$

The sub-factorization of $t_8^{\rm II(0)}$ into the convolution of a hard coefficient with the jet function is given by [34]

$$\Delta_8 C^{B1(0)}(\tau) = -\frac{eQ_d\overline{m}_b}{4\pi^2}\frac{\bar\tau}{\tau}; \qquad j_\perp^{(0)}(\tau;u,\omega) = -\frac{4\pi C_F\alpha_s}{N_c}\frac{1}{m_b\omega\bar u}\delta(\tau-u). \tag{45}$$

To show that the hard-scattering kernel $t_8^{\rm II}$ is what appears in the factorization formula (5), we now consider in more detail the hadronic matrix elements of four-quark operators in $\mathrm{SCET_{II}}$. Note that the four-quark operator whose hadronic matrix element leads to a product of LCDAs has the opposite Fierz ordering ($[\bar\xi\xi][\bar q_s h_v]$) compared to the operator whose partonic matrix element matches straightforwardly onto the expression in (43) ($[\bar\xi h_v][\bar q_s\xi]$). In four dimensions the two operators are connected by a Fierz transformation according to (see, e.g., [40])

$$O_{V_\perp} = \bar\xi \not\ell_\perp \gamma_{\nu_\perp}(1+\gamma_5) h_v\, \bar q_s \gamma^{\nu_\perp}\xi \quad \leftrightarrow \quad O'_{V_\perp} = \bar\xi \not\ell_\perp \frac{\not n_+}{2}(1+\gamma_5)\xi\, \bar q_s \frac{\not n_-}{2}\gamma_5\, h_v\,, \tag{46}$$

where the collinear (soft/HQET) fields in each operator are understood to be evaluated at different points on the $n_+(n_-)$ light-cone, and made gauge invariant by inserting appropriate Wilson lines. In writing (46) we have omitted Dirac structures contributing to $O'_{V_\perp}$ which have no projection onto the pseudoscalar B-meson LCDA. Comparing with (40), we immediately see that, in the absence of soft-collinear interactions, the hadronic matrix element of the operator $O'_{V_\perp}$ factorizes into a product of $\phi_\perp^V$ and ϕ_+^B. On the other hand, the partonic matrix element of the Fierz-transformed version $O_{V_\perp}$ matches (43), up to the hard-scattering kernel $t_8^{\rm II(0)}$. We thus verify that our expression for the tree-level amplitude is equivalent to (5).

We shall perform a similar calculation at one loop in the next subsection. A complication compared to tree level is that the appearance of IR poles in the dimensionally regulated one-loop amplitude prevents one from using the Fierz relation (46). To extract the hard-scattering kernel by comparing the renormalized matrix elements calculated in the two Fierz orderings is thus non-trivial, and will require the use of some technical details from the SCET analysis used to extract the one-loop jet function in [40, 42].

4.2 Q_8 at one loop

We now turn to a main subject of this paper, the calculation of the one-loop correction from Q_8 to the hard-scattering kernel $t^{\rm II}$. The first task is to calculate the amputated part of the full set of one-loop Feynman diagrams shown in Figure 2, supplemented by the on-shell renormalization factors for the quark fields. Photon emission from the spectator quark need not be considered for the case of pseudoscalar B-meson decay, since the four-quark structures appearing in the matching vanish at leading order in $1/m_b$ after projecting onto the meson LCDAs [34]. When a loop integral involves more than one scale, we calculate the leading term in the $1/m_b$ expansion using the method of regions. All integrals are calculated in dimensional regularization in $d = 4-2\epsilon$ dimensions and with the NDR scheme for γ_5. The result can be written in the form

$$\mathcal{A}_8^{(1)} = A^{(1)}\left(\not\ell_\perp\gamma_{\nu_\perp}\otimes\gamma_\perp^\nu\right) + B^{(1)}\left(\gamma_{\nu_\perp}\not\ell_\perp\otimes\gamma_\perp^\nu\right). \tag{47}$$

The four-quark structure multiplied by the scalar function $A^{(1)}$ is related to the matching of the operator J^{B1}. It is proportional to the tree amplitude and is used to extract the

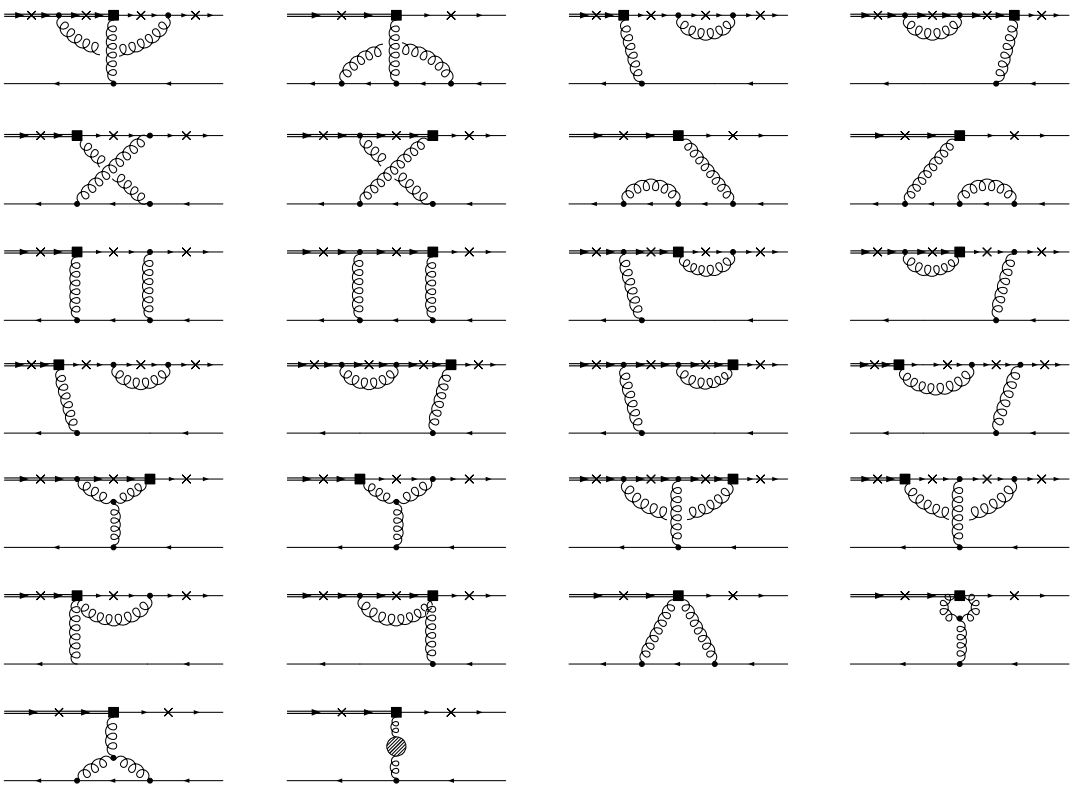

Figure 2: The one-loop corrections to spectator scattering with Q_8. The solid box denotes a Q_8 insertion and the photon can be attached to any of the crosses.

hard-scattering kernel. For our choice of external momenta, the function $A^{(1)}$ receives non-vanishing contributions from the hard, hard-collinear, and soft momentum regions. Since we work with on-shell partonic states, contributions from the collinear and soft-collinear regions are only in scaleless integrals and vanish (this would not be true if off-shell regularization were used). We shall label the contributions from the different regions as $A_h^{(1)}, A_{hc}^{(1)}$, and $A_s^{(1)}$ in what follows. Moreover, we define the amplitude $A_h^{(1)}$ to include the α_s contribution from wave-function renormalization of the b-quark field, which reads

$$Z_{2b}^{1/2} - 1 = -\frac{C_F \alpha_s}{4\pi} \left(\frac{3}{2\epsilon} + 3 \ln \frac{\mu}{m_b} + 2 \right) . \tag{48}$$

The renormalization factors for the light-quark fields vanish, to this order in α_s. In writing the result (47), we used the prescription [40]

$$\gamma^{\rho_\perp} \gamma^{\lambda_\perp} \not{\ell}_\perp \gamma^{\mu_\perp} \otimes \gamma_{\mu_\perp} \gamma_{\lambda_\perp} \gamma_{\rho_\perp} \quad \to \quad (d-4)^2 \, (\not{\ell}_\perp \gamma^{\nu_\perp} \otimes \gamma_{\nu_\perp}) \, , \tag{49}$$

the relevance of which will be explained below.

The structure multiplied by the scalar function $B^{(1)}$ is related to the matching of the operator J^{B2}. The contributions from individual diagrams contain $1/\epsilon$ poles, but these cancel in the sum of all diagrams. Since the matrix element of this four-quark operator has no projection onto the B-meson LCDA, this piece does not contribute to the hard-scattering kernel.

Note that there is no third Dirac structure, which would correspond to a contribution from the operator J^A. The matching of J^A involves the emission of the $n_+ A_{hc}$ component

of a hard-collinear gluon. Using the equations of motion $\bar{v}(k)\not{n}_+ = \not{n}_- v(\bar{u}p) = 0$ ensures that the Dirac structure can always be written in terms of the transverse components of Dirac matrices. It is easy to see that this precludes taking out a factor of $n_+ A_{hc}$ from the Wilson line in the operator J^A and attaching it to the spectator quark.

The function $A^{(1)}$ has both UV and IR divergences. The UV divergences are removed by coupling constant, mass, and operator renormalization (recall that the contribution from wave-function renormalization of the b-quark is included in the definition of $A_h^{(1)}$). We define the renormalized parameters as $\overline{m}_b^{\rm bare} = Z_m \overline{m}_b$, etc. As with the vertex term, we first compute the QCD amplitude with $n_f = n_h + n_l$ active flavors, and then express results in the $\overline{\rm MS}$ scheme in the n_l-flavor theory by renormalizing the coupling as in (17). Doing so, we find that all dependence on n_h drops out. The UV renormalized amplitude is obtained by making the replacement

$$A^{(1)} \;\to\; A^{(1)} + A^{(1)}_{\rm c.t.} = A^{(1)} + \left(Z_\alpha^{n_h+n_l(1)} + Z_m^{(1)} + Z_{88}^{(1)} - \frac{u}{\bar{u}} \frac{Z_{87}^{(1)}}{Q_d} \right) A^{(0)}, \tag{50}$$

where the various factors at one loop are

$$Z_m^{(1)} = -\frac{3 C_F \alpha_s}{4\pi\epsilon}\,, \quad Z_{88}^{(1)} = 8 \left(C_F - \frac{C_A}{4} \right) \frac{\alpha_s}{4\pi\epsilon}\,, \quad Z_{87}^{(1)} = \frac{Q_d C_F \alpha_s}{\pi\epsilon}\,. \tag{51}$$

The u-dependent factor multiplying the counterterm $Z_{87}^{(1)}$ follows from the tree-level coefficients (35,45). To this order in α_s, mass renormalization for the b-quark is needed only for the $\overline{\rm MS}$ mass appearing in the definition of Q_8, see (3).

We can extract the one-loop correction to the hard-scattering kernel from the UV renormalized partonic amplitude. It is defined by

$$\phi^{b\bar{q}'(0)} \star t_8^{\rm II(1)} \star \phi^{q\bar{q}'(0)} = A^{(1)} + A^{(1)}_{\rm c.t.} - \phi^{b\bar{q}'(1)} \star t_8^{\rm II(0)} \star \phi^{q\bar{q}'(0)} - \phi^{b\bar{q}'(0)} \star t_8^{\rm II(0)} \star \phi^{q\bar{q}'(1)}, \tag{52}$$

where the one-loop LCDAs are the renormalized ones. The one-loop contributions to the renormalized LCDAs take the form

$$\phi^{q\bar{q}'(1)} = Z_{V_\perp}^{(0)} \star \phi_{\rm bare}^{q\bar{q}'(1)} + Z_{V_\perp}^{(1)} \star \phi_{\rm bare}^{q\bar{q}'(0)}, \tag{53}$$

$$\phi^{b\bar{q}'(1)} = Z_B^{(0)} \star \phi_{\rm bare}^{b\bar{q}'(1)} + Z_B^{(1)} \star \phi_{\rm bare}^{b\bar{q}'(0)}. \tag{54}$$

The renormalization factor $Z_{V_\perp}$ for the V-meson LCDA is the Brodsky-Lepage kernel [68,69] for a transversely polarized vector meson, and that for the B-meson was calculated in [70]. Here there is an important subtlety, which is discussed in detail in [40, 42]. The renormalization factors for the B and V meson LCDAs are calculated in the $\overline{\rm MS}$ scheme under the assumption that the light-cone projection operators in (38, 39) are contracted with the specific Dirac structures shown in (40). In our case this corresponds to the one-loop corrections to the operator $O'_{V_\perp}$ in (46). However, the one-loop amplitude $A^{(1)}$ is extracted from (47) and thus multiplies the opposite Fierz ordering, corresponding to $O_{V_\perp}$ in (46). The Fierz transformation relating the two operators is valid only in $d = 4$ dimensions, and in $d = 4 - 2\epsilon$ dimensions they may differ by terms which vanish in the limit $d \to 4$. One can fix these seemingly arbitrary terms by defining a prescription for the reduction of evanescent Dirac structures, which ensures that the subtractions in (52) are performed according to the $\overline{\rm MS}$ scheme. This is achieved by using the prescription for the

evanescent operator in (49) [40, 42]. Since this structure is multiplied by poles related to the hard-collinear region, we can verify that we have performed the correct subtractions by checking eq. (59) against a corresponding result obtained using the one-loop jet function from [40, 42]. We describe this cross-check below.

To evaluate (52) it is instructive to rewrite the right-hand side as

$$\begin{aligned}(52) \;=\; & A^{(1)}_{h+hc} + A^{(1)}_{\text{c.t.}} - Z^{(1)}_B \star t_8^{\text{II}(0)} \star \phi^{q\bar{q}'(0)} - \phi^{b\bar{q}'(0)} \star t_8^{\text{II}(0)} \star Z^{(1)}_{V_\perp} \\ & + A^{(1)}_s - \phi^{b\bar{q}'(1)}_{\text{bare}} \star t_8^{\text{II}(0)} \star \phi^{q\bar{q}'(0)}. \end{aligned} \tag{55}$$

We have simplified the above equation by using that the factors $Z_i^{(0)}$ and $\phi^{i(0)}$ are delta functions, and that the one-loop correction to the bare V-meson LCDA vanishes for on-shell quarks in dimensional regularization (because the integrals are scaleless). Using the explicit results from [68–70] to perform the convolutions with the tree-level hard-scattering kernel, the first line of (55) can be written as

$$A^{(1)}_{h+hc} + A^{(1)}_{\text{c.t.}} - \left(z^{(1)}_B + z^{(1)}_{V_\perp}\right) A^{(0)}, \tag{56}$$

where

$$\begin{aligned} z^{(1)}_B &= \frac{C_F \alpha_s}{4\pi} \left[\frac{1}{\epsilon^2} + \frac{2}{\epsilon} \ln \frac{\mu}{\omega} - \frac{5}{2\epsilon}\right], \\ z^{(1)}_{V_\perp} &= \frac{C_F \alpha_s}{4\pi\epsilon} \left[-3 - \frac{2 \ln u}{\bar{u}}\right]. \end{aligned} \tag{57}$$

Evaluating (56), one finds that after UV renormalization the IR poles in the sum of the hard and hard-collinear regions are exactly subtracted by the poles related to the renormalization of the LCDAs. On the other hand, the second line of (55) vanishes, showing that contributions from the soft region are restricted to the B-meson LCDA. Therefore, the hard-scattering kernel is free of $1/\epsilon$ poles and insensitive to IR physics. This was first verified by the explicit calculations in [67].

We have shown that the finite part of the sum of hard and hard-collinear regions is $t_8^{\text{II}(1)}$. As for Q_7, we write the result as

$$t_8^{\text{II}(1)} = \Delta_8 C^{B1(0)} \star j_\perp^{(1)} + \Delta_8 C^{B1(1)} \star j_\perp^{(0)}. \tag{58}$$

We can identify the finite part of the hard-collinear region with $\Delta_8 C^{B1(0)} \star j_\perp^{(1)}$, and the finite part of the hard region with $\Delta_8 C^{B1(1)} \star j_\perp^{(0)}$. For the sum of hard-collinear graphs, we find

$$\Delta_8 C^{B1(0)} \star j_\perp^{(1)} = A^{(1)}_{\text{hc,fin}} = \frac{\alpha_s}{(4\pi)} [C_F j_F + C_A j_A + n_l j_f] t_8^{\text{II}(0)}, \tag{59}$$

where $n_l = 4$ is the number of light flavors, and ($L_{\rm hc} = \ln m_b\omega/\mu^2$)

$$\begin{aligned}
j_F &= L_{\rm hc}^2 + \left(5 - \frac{2-2\ln u}{\bar u} + 2\ln u\right) L_{\rm hc} + \frac{4}{\bar u} - 12 - \frac{\pi^2}{6} \\
&\quad + \left(5 - \frac{4}{\bar u}\right)\ln\bar u + \frac{2\ln\bar u\ln u}{\bar u} + \ln^2 u\left(1+\frac{1}{\bar u}\right) + \frac{4}{\bar u}{\rm Li}_2(\bar u), \\
j_A &= \left(-\frac{11}{3} + \ln\bar u - \left(1+\frac{1}{\bar u^2}\right)\ln u\right) L_{\rm hc} + \frac{76}{9} + \left(-\frac{11}{3}+\frac{1}{\bar u}\right)\ln\bar u + \frac{\ln^2\bar u}{2}, \\
&\quad + \left(\frac{1}{\bar u^2} - \frac{1}{\bar u}\right)\ln u - \left(\frac{1}{2} + \frac{1}{2\bar u^2}\right)\ln^2 u - \frac{\ln\bar u\ln u}{\bar u^2} - \frac{2}{\bar u^2}{\rm Li}_2(\bar u), \\
j_l &= \frac{2}{3}L_{\rm hc} + \frac{2\ln\bar u}{3} - \frac{10}{9}.
\end{aligned} \tag{60}$$

Taking the convolution of the one-loop jet function $j_\perp^{(1)}$ listed in the Appendix with the leading-order hard coefficient in (45), we reproduce the above equation. This verifies that the sub-factorization of the hard-scattering kernel according to momentum regions is equivalent to that in SCET, and also that we have performed the correct subtractions in (52). However, we again emphasize that this integrated form cannot be used to obtain the resummed hard-scattering kernels used in our numerical analysis in Section 5.

The finite part of the hard region gives an expression for $\Delta_8 C^{B1(1)} \star j_\perp^{(0)}$. In this case we have

$$\Delta_8 C^{B1(1)} \star j_\perp^{(0)} = A_{\rm h,fin}^{(1)} = \frac{\alpha_s}{4\pi}[C_F h_F + C_A h_A] t_8^{\rm II(0)}\,, \tag{61}$$

where

$$\begin{aligned}
h_F &= -2L^2 - \left(1 + \frac{4}{\bar u} - 4\ln u\right) L - \left(18 - \frac{8}{\bar u}\right) L_{\rm QCD} + i\pi\left(-4 + \frac{2}{\bar u} + \frac{2\ln u}{\bar u^2}\right) \\
&-15 + \frac{7\pi^2}{12} - \frac{1}{\bar u} - \frac{2\pi^2}{3\bar u} + \left(2 + \frac{2}{u} + \frac{4}{\bar u}\right)\ln\bar u \\
&+ \left(4 - \frac{2}{\bar u} - \frac{2}{\bar u^2}\right)\ln u + \left(\frac{3}{\bar u} + \frac{2}{\bar u^2} + \frac{1}{2-\bar u}\right)\ln\bar u\ln u - \left(2 + \frac{1}{\bar u^2}\right)\ln^2 u \\
&+ \left(-2 + \frac{1}{2\bar u} + \frac{3}{\bar u^2} + \frac{1}{2(2-\bar u)}\right){\rm Li}_2(\bar u) + \left(\frac{5}{\bar u} - \frac{6}{\bar u^2} + \frac{1}{2-\bar u}\right) g(\bar u) + \left(\frac{1}{\bar u} - \frac{1}{2-\bar u}\right) h(\bar u), \\
h_A &= \left(-2\ln u - \frac{2\ln u}{\bar u^2} + 2\ln\bar u\right) L + 4L_{\rm QCD} + i\pi\left(1 - \frac{1}{\bar u} - \frac{2\ln u}{\bar u^2}\right) + 2 - \frac{\pi^2}{3} + \frac{3}{\bar u} \\
&- \frac{\ln\bar u}{\bar u} + \left(-1 + \frac{2}{\bar u} - \frac{1}{\bar u^2}\right)\ln u + \left(1 - \frac{3}{2\bar u} - \frac{1}{2(2-\bar u)}\right)\ln\bar u\ln u - \ln^2\bar u \\
&+ \left(1 + \frac{1}{\bar u^2}\right)\ln^2 u + \left(2 - \frac{1}{4\bar u} - \frac{1}{2\bar u^2} - \frac{1}{4(2-\bar u)}\right){\rm Li}_2(\bar u) \\
&+ \left(-\frac{5}{2\bar u} + \frac{3}{\bar u^2} - \frac{1}{2(2-\bar u)}\right) g(\bar u) + \left(-\frac{1}{2\bar u} + \frac{1}{2(2-\bar u)}\right) h(\bar u).
\end{aligned} \tag{62}$$

The logarithms L and $L_{\rm QCD}$ are defined after (21). The terms proportional to L agree with the corresponding terms in [67], and can be deduced by convoluting the renormalization factor $z_\perp(\tau)$ of the SCET current J^{B1} obtained in [40, 41] with the tree-level hard

coefficient $\Delta_8 C^{B1}$ in (45). We have defined the functions

$$g(u) = \int_0^1 dy\, \frac{\ln[1-uy(1-y)]}{y}, \tag{63}$$

$$h(u) = \int_0^1 dy\, \frac{\ln[1-uy(1-y)]}{1-uy}. \tag{64}$$

These functions have no imaginary part for $u \in [0,1]$ and can be expressed in terms of dilogarithms and logarithms, but we shall not give the explicit results here. Since $j_\perp^{(0)}$ is a delta function in τ, the result for $\Delta_8 C^{B1(1)}$ is obtained directly from (62).

5 Numerical analysis

In this section we discuss the numerical impact of our results. Our main focus is on the branching fractions for $B \to K^*\gamma$ and $B_s \to \phi\gamma$ decays. The branching fraction for $B \to K^*\gamma$ decays is

$$\mathcal{B}(B \to K^*\gamma) = \frac{\tau_B m_B}{4\pi}\left(1 - \frac{m_{K^*}^2}{m_B^2}\right)\left|\mathcal{A}_{\rm v} + \mathcal{A}_{\rm hs}\right|^2 , \tag{65}$$

where we have split the contributions from the vertex and hard-spectator corrections according to

$$\mathcal{A}_{\rm v} = \frac{G_F}{\sqrt{2}} V_{cs}^* V_{cb} \sum_i C_i(\mu_{\rm QCD})\, \Delta_i C^A(m_b, \mu_{\rm QCD}, \mu)\zeta_{K_\perp^*}(\mu), \tag{66}$$

$$\mathcal{A}_{\rm hs} = \frac{G_F}{\sqrt{2}} V_{cs}^* V_{cb} \sum_i C_i(\mu_{\rm QCD})\, t_i^{\rm II}(\mu_{\rm QCD}, \mu) \star \left(\frac{\sqrt{m_B}F}{4}\phi_+^B \star f_{K^*}\phi_{K_\perp^*}\right)(\mu). \tag{67}$$

Results for $B_s \to \phi\gamma$ are obtained by making the appropriate replacements. The branching fractions depend on a number of parameters, whose values and uncertainties are summarized in Table 3. The vertex and hard-spectator amplitudes are independently invariant under variations of $\mu_{\rm QCD}$ and μ. For this reason, their contributions to the amplitudes can be studied separately. We discuss each one in turn for the case of $B \to K^*\gamma$, before presenting the final branching fractions for all decay modes in Section 5.4.

5.1 The vertex amplitude

We begin with the vertex corrections. For these corrections the relevant perturbative quantities are the Wilson coefficients C_i in the effective weak Hamiltonian and the SCET matching coefficients $\Delta_i C^A$. We calculate the Wilson coefficients in the effective weak Hamiltonian using the information summarized in Appendix A of [16] (see also [12, 13]), and collect the results for three values of the renormalization scale in Table 2. The results for the SCET matching coefficients are simplest when $\mu_{\rm QCD} = \mu = m_b$, in which case all logarithms vanish. We use this choice as our default scheme. Throughout the analysis we use the four-loop running coupling with $\alpha_s(m_Z) = 0.1176$, switching from five to four active flavors at the matching scale $\mu_h = \mu_{\rm QCD}$. The vertex amplitude and the branching fractions depend rather strongly on $\zeta_{V_\perp}$. We determine it in Section 5.3 by

requiring that the matrix element of Q_7 be proportional to the QCD form factor $F^{B\to V_\perp}$ at NNLO, finding $\zeta_{V_\perp}(\mu = m_b) = 0.35 \pm 0.05$. We will express higher-order corrections to the amplitudes in terms of the leading-order result, which is

$$\mathcal{A}_{\rm v}^{\rm LO} = -\frac{G_F}{\sqrt{2}} V_{cs}^* V_{cb} C_7^{LL} \frac{e\,\overline{m}_b\, 2E_\gamma}{4\pi^2} \zeta_{K_\perp^\star} = -5.48 \times 10^{-9}\,. \tag{68}$$

Up to NNLO, the result obtained using the default parameter values in Table 3 is

$$\frac{\mathcal{A}_{\rm v}^{\rm NNLO}}{\mathcal{A}_{\rm v}^{\rm LO}} = 1 + (0.096 + 0.057i)\,[\alpha_s] + (-0.007 + 0.030i)\,\left[\alpha_s^2\right], \tag{69}$$

where the first term in parentheses is the NLO (α_s) correction and the second term the NNLO (α_s^2) correction. The corrections come both from the Wilson coefficients C_i in the effective weak Hamiltonian and the SCET coefficients $\Delta_i C^A$. Note that we have used the effective coefficients $C_{7,8}^{\rm eff}$ in the numerical analysis. This amounts to including certain contributions from $Q_3 \ldots Q_6$, and should be taken into account, if in the future the contributions from these operators are worked out systematically. Split into contributions from the individual operators, the results for the NLO and NNLO perturbative corrections read

$$\begin{aligned}
\frac{\mathcal{A}_{\rm v}^{\rm NNLO}}{\mathcal{A}_{\rm v}^{\rm LO}} - 1 &= \Big((0.264 + 0.034i)\,[Q_1] - (0.184)\,[Q_7] + (0.016 + 0.023i)\,[Q_8]\Big)\,[\alpha_s] \\
&+ \Big((0.073 + 0.022i)\,[Q_1] - (0.081)\,[Q_7] + (0.002 + 0.008i)\,[Q_8]\Big)\,[\alpha_s^2]\,.
\end{aligned} \tag{70}$$

At both NLO and NNLO the corrections from Q_1 and Q_7 are relatively large, but the real parts tend to cancel against each other. Whether this cancellation persists beyond the large-β_0 limit is an important question. The contribution from Q_8 to the real part of the amplitude is small, but that to the imaginary part is not. It adds together with that from Q_1 to produce a large NNLO correction to the imaginary part. This would be a significant effect for CP asymmetries, a topic we leave for future work.

In Section 5.4 we will study the dependence of the branching fractions on the renormalization scales. To do this we use the SCET Wilson coefficients as given in (30) in Section 3. As explained there, this allows us to fix the scale $\mu = m_b$ in $\zeta_{V_\perp}$ and study the stability of the results under variations in $\mu_{\rm QCD}$ and μ_h. Although the expressions in the Appendix allow us to vary $\mu_{\rm QCD}$ and μ_h separately, we choose not to do so. For simplicity, we set $\mu_{\rm QCD} = \mu_h$ and vary them simultaneously. To evaluate the RG exponents in the SCET evolution factors we distinguish the operators $Q_{7,8}$ and Q_1. For $Q_{7,8}$ we evaluate the RG exponents using the two-loop anomalous dimensions in a and a_J, and the three-loop cusp anomalous dimension in the Sudakov factor S. For Q_1 we evaluate the RG exponents using the large-β_0 limit. In that case it is consistent to set all SCET anomalous dimensions to zero, meaning that we can use the form (29) directly.

5.2 The hard spectator amplitude

The evaluation of the hard spectator amplitude is more complicated than the vertex amplitude. It involves a large number of hadronic parameters and the hard-scattering kernel contains logarithms of both the hard and hard-collinear scales. While it is possible

Table 2: Wilson coefficients $C_i(\mu)$ $(i = 1, 7, 8)$ at LL, NLL and NNLL. The results at NNLL are calculated from the expressions given in [12, 13, 16], adapted to the operator basis in (2, 3). The table uses $m_b = 4.8$ GeV.

	LL	NLL	NNLL
$C_1(\mu = m_b)$	1.11	1.06	
$C_1(\mu = \sqrt{2}m_b)$	1.09	1.04	
$C_1(\mu = m_b/\sqrt{2})$	1.13	1.08	
$C_7^{\rm eff}(\mu = m_b)$	-0.312	-0.303	-0.294
$C_7^{\rm eff}(\mu = \sqrt{2}m_b)$	-0.294	-0.290	-0.282
$C_7^{\rm eff}(\mu = m_b/\sqrt{2})$	-0.332	-0.316	-0.306
$C_8^{\rm eff}(\mu = m_b)$	-0.148	-0.167	
$C_8^{\rm eff}(\mu = \sqrt{2}m_b)$	-0.141	-0.159	
$C_8^{\rm eff}(\mu = m_b/\sqrt{2})$	-0.156	-0.175	

to fix the scale $\mu_{\rm QCD} \sim m_b$ to eliminate some of these logarithms, any choice of the SCET factorization scale μ leads to large logarithms in $t_i^{\rm II}$. This can be solved by renormalization-group improvement in the effective theory [41]. The hard coefficient $\Delta_i C^{B1}$ is extracted at a scale $\mu_h \sim \mu_{\rm QCD} \sim m_b$ and and evolved down to the intermediate scale $\mu_i \sim 1.5$ GeV by solving the RG equations in the effective theory. The RG-improved hard coefficients read [41]

$$\Delta_i C^{B1}(u, \mu_i) = \left(\frac{m_b}{\mu_h}\right)^{a(\mu_h,\mu_i)} e^{S(\mu_h,\mu_i)} \int_0^1 dv\, U_\perp(u, v, \mu_h, \mu_i) \Delta_i C^{B1}(v, \mu_h)\,. \tag{71}$$

The RG exponents S and a are the same as in (31). The evolution factor $U_\perp$ is the solution to the integro-differential equation

$$\mu \frac{d}{d\mu} U_\perp(u, v, \mu_h, \mu) = \int_0^1 dy\, \gamma_\perp(y, u) U_\perp(y, v, \mu_h, \mu), \tag{72}$$

with the initial condition $U_\perp(u, v, \mu_h, \mu_h) = \delta(u - v)$. The distribution $\gamma_\perp(y, u)$ is the anomalous dimension of the operator J^{B1}. A proper treatment of the NNLO matching corrections requires this anomalous dimension at two loops, but at present it is known only at one loop [40,41]. This adds a small uncertainty to the analysis. The solution to the evolution equation is obtained numerically. In the numerical implementation we perform the μ-evolution from μ_h to μ_i in 100 discrete steps. We choose the default renormalization scales as $\mu_{\rm QCD} = \mu_h = m_b$ and $\mu_i = 1.5$ GeV. The dependence on the variable u in the resummed $\Delta_i C^{B1}$ is obtained for discretized values of $0 < u < 1$. We determine the discretization scale by taking more points in u until the numerical convolution of the resummed coefficient with the jet function becomes stable. This generally requires between one and three-hundred values, although for some cases it is necessary to take more values near the endpoints.

It is natural to evaluate the resummed hard coefficients $\Delta_i C^{B1}(u, \mu)$ at a scale $\mu \sim \mu_i$, since at that scale the jet function is free of large logs. However, the hadronic parameters in Table 3 are extracted at a low scale $\mu = 1$ GeV. For a proper treatment one must

either run these parameters up to the intermediate scale $\mu_i \sim 1.5$ GeV, or run the hard-scattering kernel down to the lower scale. This stage of RG running has been studied in [41,70,71]. We have performed this evolution in our numerical analysis but its effect on the branching fractions is extremely small. Therefore, in quoting our results, we perform the running from μ_h to μ_i, but ignore that between the scale μ_i and the factorization scale $\mu \sim 1$ GeV. The shortcoming of this treatment is that the amplitude is not invariant under variations of the intermediate scale. However, the dominant effect in this scale variation is related the B-meson distribution amplitude. We account for this in our error analysis by assigning a rather large uncertainty to λ_B.

A complete treatment of the hard-spectator amplitude is only possible for the NLO corrections. There are three pieces missing for a full resummed result for the hard-spectator term at NNLO: the NNLO hard matching coefficient for Q_1, the two-loop anomalous dimension of the current J^{B1}, and the two-loop anomalous dimension of the jet function. These missing pieces add uncertainties to the analysis which are difficult to quantify. However, we will see that the higher-order corrections from spectator scattering are not very important for the branching fractions.

In addition to the input parameters listed in Table 3, we must also specify the meson LCDAs. For the vector mesons we use the Gegenbauer expansion and keep only the first two moments:

$$\phi_V(u) = 6u(1-u)\left[1 + a_1^V(\mu) C_1^{(3/2)}(2u-1) + a_2^V(\mu) C_2^{(3/2)}(2u-1)\right]. \tag{73}$$

For the B-meson LCDA we use the model [72]

$$\phi_+^B(\omega, \mu = 1\,\text{GeV}) = \frac{4\lambda_B^{-1}}{\pi} \frac{\omega\,\mu}{\omega^2+\mu^2}\left[\frac{\mu^2}{\omega^2+\mu^2} - \frac{2(\sigma_B - 1)}{\pi^2}\ln\frac{\omega}{\mu}\right]. \tag{74}$$

The B-meson decay constant in the static limit is

$$F(\mu) = \frac{f_B\sqrt{m_B}}{K(\mu_h)} e^{V_F(\mu_h,\mu)}\,, \tag{75}$$

where to one loop [73]

$$K_F(\mu) = 1 + \frac{C_F\alpha_s(\mu)}{4\pi}\left(3\ln\frac{m_b}{\mu} - 2\right), \qquad V_F(\mu_h,\mu) = -\frac{3C_F}{2\beta_0}\ln\frac{\alpha_s(\mu)}{\alpha_s(\mu_h)}. \tag{76}$$

We now quote the result for the hard-spectator amplitude to NNLO, accurate within the limitations explained above. We find

$$\frac{\mathcal{A}_{\rm hs}^{\rm NNLO}}{\mathcal{A}_{\rm v}^{\rm LO}} = \big(0.11 + 0.05i\big)\,[\alpha_s] + \big(0.03 + 0.01i\big)\,[\alpha_s^2]. \tag{77}$$

Performing the RG evolution of the hard-scattering kernel between μ_i and the factorization scale $\mu = 1$ GeV suppresses the above result by about 10%, or in other words makes about a 1% difference on the total amplitude. Split into contributions from the individual operators, we have

$$\begin{aligned}\frac{\mathcal{A}_{\rm hs}^{\rm NNLO}}{\mathcal{A}_{\rm v}^{\rm LO}} &= \Big((0.023 + 0.046i)\,[Q_1] + 0.074\,[Q_7] + 0.010\,[Q_8]\Big)\,[\alpha_s] \\ &+ \Big((0.004 + 0.003i)\,[Q_1] + 0.025\,[Q_7] + (0.003 + 0.005i)\,[Q_8]\Big)\,[\alpha_s^2]\,.\end{aligned} \tag{78}$$

Unlike the case of the vertex corrections, the individual contributions from the different operators are rather small at NLO and especially NNLO. For Q_1 we have listed the NNLO correction found by numerically evaluating $\Delta_1 C^{B1(0)} \star j_\perp^{(1)}$. In addition to this correction from the jet function, there is also a hard correction $\Delta_1 C^{B1(1)} \star j_\perp^{(0)}$ which is not known. Both terms are used for Q_7 and Q_8. To check the convergence of perturbation theory at the intermediate scale $\mu_i \sim 1.5$ GeV we split up the contributions from each operator into these two contributions. We also separate the NNLO corrections from the Wilson coefficients in the effective weak Hamiltonian separate, labeling them with a [w]. For these three sources of NNLO corrections, in units of $1/A_{\rm v}^{\rm LO}$, we have

$$\begin{aligned}
Q_1 &: (0.023 + 0.046i)\,[\alpha_s] + \Big((-0.001 - 0.002i)\,[\mathrm{w}] + (0.005 + 0.006i)\,[\mathrm{jet}]\Big)\,[\alpha_s^2],\\
Q_7 &: 0.074\,[\alpha_s] + \Big(-0.002\,[\mathrm{w}] + 0.015\,[\mathrm{jet}] + 0.012\,[\mathrm{hard}]\Big)\,[\alpha_s^2],\\
Q_8 &: 0.01\,[\alpha_s] + \Big(0.001\,[\mathrm{w}] + 0.001\,[\mathrm{jet}] + (0.001 + 0.005i)\,[\mathrm{hard}]\Big)\,[\alpha_s^2].
\end{aligned} \tag{79}$$

In none of the cases is the correction at the jet scale $\mu_i = 1.5$ GeV unusually large.

5.3 The SCET soft function

In this subsection we explain our method for determining the SCET soft function $\zeta_{V_\perp}$. We fix it by requiring that the matrix element of Q_7 is proportional to the tensor QCD form factor $F^{B\to V_\perp}$ (often referred to as T_1). Using the SCET factorization formula for Q_7 we find

$$F^{B\to V_\perp} = \frac{\Delta_7 C^A}{\Delta_7 C^{A(0)}}\zeta_{V_\perp} - \frac{1}{\Delta_7 C^{B1(0)}} t_7^{\rm II} \star \left(\frac{\sqrt{m_B}F}{4m_b}\phi_B \star f_{V_\perp}\phi_{V_\perp}\right). \tag{80}$$

The recent LCSR-based update [25] for the tensor QCD form factor yields $F^{B\to K^*} = F^{B\to\phi} = 0.31 \pm 0.04$ at $\mu_{\rm QCD} = m_b$. Inserting this into (80) and treating the hard-spectator term as in the default scheme above leads to $\zeta_{V_\perp}(\mu = m_b) = 0.35 \pm 0.05$. This is considerably smaller than the value $\zeta_{V_\perp} \simeq 0.41$ used in the SCET analysis in [34], and it is mainly for this reason that we find smaller branching fractions below.

We can use this value for $\zeta_{V_\perp}$ to compare the size of higher-order corrections to the factorization formula for the form factor. We label the vertex term (v) and the hard spectator term (hs), and express each as an expansion in α_s. Then the individual contributions read

$$\frac{F^{B\to V_\perp}}{\zeta_{V_\perp}} = \big(1 - 0.15[\alpha_s] - 0.06[\alpha_s^2]\big)[\mathrm{v}] + \big(0.07[\alpha_s] + 0.03[\alpha_s^2]\big)[\mathrm{hs}]\,. \tag{81}$$

For both the α_s and α_s^2 corrections the vertex term is about twice as large as the hard-spectator term and comes with the opposite sign.

5.4 Branching fractions

We now convert our results for the amplitudes into estimates for the branching fractions at NNLO. The most important uncertainties in the input parameters come from $\zeta_{V_\perp}$, $\sqrt{z} =$

Table 3: Input parameters used in the calculation of $\mathcal{B}(B \to K^*\gamma)$ and $\mathcal{B}(B \to \phi\gamma)$. The Gegenbauer coefficients in the LCDAs are taken from the LCSR analysis reported in [25].

Parameter	Value
$\alpha_s(m_Z)$	0.1176
$V_{cs}^* V_{cb}$	-0.040 ± 0.002
$\zeta_{K^*\perp}(0)$	0.35 ± 0.05
$\zeta_{\phi_\perp}(0)$	0.35 ± 0.05
$m_{b,\rm pole}$	(4.80 ± 0.10) GeV
$m_{t,\rm pole}$	(171 ± 2.0) GeV
$\sqrt{z} = m_c/m_b$	0.27 ± 0.06
f_B	(205 ± 25) MeV
f_{B_s}	(240 ± 30) MeV
$f_\perp^{(K^*)}(1\text{ GeV})$	(185 ± 10) MeV
$f_\perp^{(\phi)}(1\text{ GeV})$	(186 ± 9) MeV
$a_{\perp 1}^{(K^*)}(1\text{ GeV})$	0.04 ± 0.03
$a_{\perp 1}^{(\phi)}(1\text{ GeV})$	0.0
$a_{\perp 2}^{(K^*)}(1\text{ GeV})$	0.15 ± 0.10
$a_{\perp 2}^{(\phi)}(1\text{ GeV})$	0.20 ± 0.20
$\lambda_B^{-1}(1\text{ GeV})$	(2.15 ± 0.50) GeV^{-1}
$\sigma_B(1\text{ GeV})$	(1.4 ± 0.4)

m_c/m_b, λ_B, and the renormalization scales. To assess the uncertainty associated with $\zeta_{V_\perp}$, m_c and λ_B, we vary them in the ranges indicated in Table 3. The scale dependence of the branching fraction is completely dominated by the vertex term. We treat this dependence as explained in Section 5.1, varying the scale $\mu_h = \mu_{\rm QCD}$ in the range $m_b/\sqrt{2} < \mu_h < \sqrt{2} m_b$. Including the corrections up to NNLO and discarding terms of $\mathcal{O}(\alpha_s^3)$ and higher in the branching fractions, we find

$$\begin{aligned}
\mathcal{B}(B^+ \to K^{*+}\gamma) &= (4.6 \pm 1.2\,[\zeta_{K^*}] \pm 0.4\,[m_c] \pm 0.2\,[\lambda_B] \pm 0.1\,[\mu]) \times 10^{-5}, \\
\mathcal{B}(B^0 \to K^{*0}\gamma) &= (4.3 \pm 1.1\,[\zeta_{K^*}] \pm 0.4\,[m_c] \pm 0.2\,[\lambda_B] \pm 0.1\,[\mu]) \times 10^{-5}, \\
\mathcal{B}(B_s \to \phi\gamma) &= (4.3 \pm 1.1\,[\zeta_\phi] \pm 0.3\,[m_c] \pm 0.3\,[\lambda_B] \pm 0.1\,[\mu]) \times 10^{-5}. \qquad (82)
\end{aligned}$$

In cases where the errors are asymmetric, we have taken the average of the higher and lower values to get the symmetric form above. The uncertainty in $|V_{cs}^* V_{cb}|$, which appears as an overall factor multiplying the branching fractions, adds about a 10% error to each decay mode. To obtain the branching fractions we used the following lifetimes (in units of ps) [7]

$$\tau(B^0) = 1.527 \pm 0.008; \quad \tau(B^+) = 1.643 \pm 0.010; \quad \tau(B_s) = 1.451 \pm 0.028\ . \qquad (83)$$

In addition to the lifetime differences, our analysis of the three decay modes includes differences in the meson decay constants, meson masses, and Gegenbauer moments of the light-meson LCDAs (we have assumed that SU(3) violating effects in the B-meson LCDAs are small). Other sources of isospin and SU(3) violation are not included. Concerning

the ϕ and K^* decay modes, the most important source of SU(3) violation is the difference between the SCET soft functions of the two mesons. We discuss this in more detail below, giving a result for the ratio of branching fractions of these two decay modes. A study of dynamical isospin breaking contributions within QCD factorization was carried out in [20]. From this study we expect the dynamical isospin violating effects to make only a small difference in the branching fractions.

It is important to keep in mind that we have not completed the NNLO calculation for Q_1. The NNLO vertex correction is only an estimate in the large-β_0 limit and the NNLO hard-spectator correction related to $\Delta_1 C^{B1}$ is entirely absent. To study the effects of possible deviations from large-β_0 limit we assign a 100% uncertainty to the NNLO vertex correction from Q_1, evaluating the branching fractions using $2\Delta_1 C^{A(2)}$ and $\Delta_1 C^{A(2)} = 0$. For the hard spectator term we take the NNLO correction as ± 1 its NLO value. The corresponding uncertainties in the branching fractions, to be added to the errors quoted in (82), are ± 0.5 for the vertex corrections and ± 0.1 for the hard-spectator corrections. The uncertainties associated with the unknown corrections to hard spectator scattering make little difference for the branching fraction. The uncertainties associated with the large-β_0 limit in the vertex term are rather large, even though this is an $\mathcal{O}(\alpha_s^2)$ correction. We are very conservative with the range in which we vary this correction, but even in the only existing calculation of NNLO corrections from Q_1 beyond the large-β_0 limit [53] for the inclusive case this is an issue. In that paper the part of the $O(\alpha_s^2)$ correction to the matrix element of Q_1 beyond the large-β_0 limit (called $P_2^{(2)\mathrm{rem}}(z_0)$ in [53]) remains rather uncertain.

Adding together all the errors mentioned above in quadrature, we obtain the final results for the branching fractions

$$\begin{aligned}
\mathcal{B}(B^+ \to K^{*+}\gamma) &= (4.6 \pm 1.4) \times 10^{-5}, \\
\mathcal{B}(B^0 \to K^{*0}\gamma) &= (4.3 \pm 1.4) \times 10^{-5}, \\
\mathcal{B}(B_s \to \phi\gamma) &= (4.3 \pm 1.4) \times 10^{-5}.
\end{aligned} \tag{84}$$

The NNLO estimates given in (84) are to be compared with the experimental measurements summarized in Table 1. We find

$$\begin{aligned}
\frac{\mathcal{B}(B^+ \to K^{*+}\gamma)_{\mathrm{SM,NNLO}}}{\mathcal{B}(B^+ \to K^{*+}\gamma)_{\mathrm{expt}}} &= 1.1 \pm 0.35\,[\mathrm{theory}] \pm 0.07\,[\mathrm{expt.}]\,, \\
\frac{\mathcal{B}(B^0 \to K^{*0}\gamma)_{\mathrm{SM,NNLO}}}{\mathcal{B}(B^0 \to K^{*0}\gamma)_{\mathrm{expt}}} &= 1.1 \pm 0.35\,[\mathrm{theory}] \pm 0.06\,[\mathrm{expt.}]\,, \\
\frac{\mathcal{B}(B_s \to \phi\gamma)_{\mathrm{SM,NNLO}}}{\mathcal{B}(B_s \to \phi\gamma)_{\mathrm{expt}}} &= 0.8 \pm 0.2\,[\mathrm{theory}] \pm 0.3\,[\mathrm{expt.}]\,.
\end{aligned} \tag{85}$$

Although the results are in reasonable agreement with each other, the theory errors for the $B \to K^*\gamma$ decay modes are still much larger than the experimental ones. The dominant uncertainty is in the SCET soft function $\zeta_{V_\perp}$. The remaining uncertainties would be greatly reduced by determining the NNLO corrections from Q_1 to the vertex term beyond the large-β_0 limit. This would not only directly eliminate the uncertainty in the NNLO correction to the hard-scattering kernel, it would also reduce the dependence on the charm-quark mass by fixing its perturbative definition.

Another measurement of interest is the ratio of the branching fractions of the K^* and ϕ decay modes. In the ratio, only the errors in the quantities which are different for

the B_s, ϕ and B, K^* mesons add significant uncertainties. Since the spectator scattering amplitude is small compared to the vertex term, to a good approximation the error is given by that in the ratio ζ_{K^*}/ζ_ϕ. As an example, assuming $\zeta_{K^*}/\zeta_\phi = 1 \pm 0.1$, we find for the ratio of branching fractions

$$\frac{\mathcal{B}(B^0 \to K^{*0}\gamma)}{\mathcal{B}(B_s \to \phi\gamma)} = 1.0 \pm 0.2\,. \tag{86}$$

By comparison, the current experimental number is 0.7 ± 0.3. Improved measurements of the $B_s \to \phi\gamma$ branching fraction, and a more accurate determination of the ratio of SCET soft functions, would allow for a comparison between theory and experiment with smaller uncertainties than for the branching fractions themselves.

6 Conclusions

We computed NNLO corrections to the hard-scattering kernels entering the QCD factorization formula for $B \to V\gamma$ decays. We used soft-collinear effective theory to separate contributions between the hard and hard-collinear scales and to resum large logarithms depending on their ratio. For the operators Q_7 and Q_8 we obtained exact expressions for the hard-scattering kernels for the vertex and hard spectator corrections up to NNLO. The results for the vertex corrections provide an explicit demonstration of factorization at two loops. For the operator Q_1, we estimated its contribution to the vertex correction at NNLO using the large-β_0 limit. Its complete NNLO correction from hard spectator scattering was not obtained, but its contribution at the jet scale was evaluated numerically and found to be small.

As an application of our results we provided estimates of the branching fractions for $B \to K^*\gamma$ and $B_s \to \phi\gamma$ decays at NNLO. The branching fractions are very sensitive to the value of the SCET soft function $\zeta_{V_\perp}$. We used updated results from QCD sum rules for the tensor form factor $F^{B\to V_\perp}$ along with our NNLO results for Q_7 to find $\zeta_{V_\perp} \simeq 0.35$. Since this value is considerably lower than the default value $\zeta_{V_\perp} \simeq 0.41$ used in the previous SCET analysis in [34], we also find lower branching fractions. Our results for the $B \to K^*\gamma$ modes show good agreement with the experimental data, but the theory errors are still much larger than the experimental ones. Our result for $B_s \to \phi\gamma$, which has a comparable theoretical error as in the $B \to K^*\gamma$ modes, is also in agreement with the data within the large experimental error. The main theoretical uncertainty is in $\zeta_{V_\perp}$, which can be reduced by improved lattice or QCD sum-rule calculations. On the perturbative side, by far the most important issue is the calculation of the NNLO vertex correction for Q_1 beyond the large-β_0 limit. This requires the same diagrammatic calculation as the virtual corrections to inclusive $B \to X_s\gamma$, which remains to be done. Our results are also relevant for $B \to \rho\gamma$ and $B \to \omega\gamma$, but for these decays a complete description also requires the perturbative corrections to weak annihilation, a topic we leave for future work.

Acknowledgments: We would like to thank Alexander Parkhomenko for collaboration in the early stages of this work, Guo-huai Zhu for correspondence on the numerical aspects of SCET resummation, and Thomas Becher for useful discussions. One of us (C.G.) thanks DESY for the hospitality in Hamburg where this work was carried out. This work was supported in part by the EU Contract No. MRTN-CT-2006-035482, FLAVIAnet.

7 Appendix

7.1 Matrix elements

In the section we give results for the UV renormalized on-shell matrix elements

$$\langle Q_i\rangle \equiv \langle q(p)\gamma(q)|Q_i|b(p_b)\rangle$$

in QCD. The results given below are calculated in the $\overline{\rm MS}$ renormalization scheme with $n_f = n_h + n_l$ flavors. For Q_7 and Q_8 we write

$$\langle Q_i\rangle = \langle Q_{7,tree}\rangle \left[\delta_{i7} + \frac{C_F\alpha_s}{4\pi}D_i^{(1)} + \left(\frac{\alpha_s}{4\pi}\right)^2 C_F\left(C_F D_{iF}^{(2)} + C_A D_{iA}^{(2)} + n_l D_{iL}^{(2)} + n_h D_{iH}^{(2)}\right)\right]. \tag{87}$$

For Q_7 the results are [43, 44] (recall $L = \ln\mu/m_b$)

$$\begin{aligned}
D_7^{(1)} &= -\frac{1}{\epsilon^2} - \frac{2L+2.5}{\epsilon} - 2L^2 - 7L - 6.8225 \\
&\quad -\epsilon(1.3333L^3 + 7L^2 + 13.6449L + 13.4779) \\
&\quad -\epsilon^2(0.6667L^4 + 4.6667L^3 + 13.6449L^2 + 26.9559L + 26.1412), \\
D_{7F}^{(2)} &= \frac{0.5}{\epsilon^4} + \frac{2L+2.5}{\epsilon^3} + \frac{4L^2+12L+9.9475}{\epsilon^2} + \frac{5.3333L^3+26L^2+44.7899L+27.8816}{\epsilon} \\
&\quad +5.3333L^4 + 36L^3 + 96.5798L^2 + 144.1712L + 67.6519, \\
D_{7A}^{(2)} &= \frac{2.75}{\epsilon^3} + \frac{3.6667L+3.5447}{\epsilon^2} - \frac{4.1546L+3.4386}{\epsilon} \\
&\quad -4.8889L^3 - 33.9758L^2 - 92.3415L - 83.8866, \\
D_{7L}^{(2)} &= -\frac{0.5}{\epsilon^3} - \frac{0.6667L+0.5556}{\epsilon^2} + \frac{1.1111L+1.9799}{\epsilon} \\
&\quad +0.8889L^3 + 6.8889L^2 + 19.9050L + 23.8254, \\
D_{7H}^{(2)} &= \frac{1.3333L}{\epsilon^2} + \frac{4L^2+3.3333L+0.5483}{\epsilon} + 6.2222L^3 + 11.3333L^2 + 14.1788L + 0.2934,
\end{aligned} \tag{88}$$

and for Q_8 we have [45]

$$\begin{aligned}
D_8^{(1)} &= 2.6667L + 1.4734 + 2.0944i + \epsilon[2.6667L^2 + 2.9468L - 1.1947 + i(4.1888L + 4.1888)] \\
&\quad +\epsilon^2[1.7778L^3 + 2.9468L^2 - 2.3894L - 5.5373 + i(4.1888L^2 + 8.3776L + 2.1627)], \\
D_{8F}^{(2)} &= D_8^{(1)}\left(-\frac{1}{\epsilon^2} - \frac{2L+2.5}{\epsilon}\right) - 5.3333L^3 - 32.2802L^2 - 50.9612L - 1.8875 \\
&\quad -i(4.1888L^2 + 31.4159L + 29.8299), \\
D_{8A}^{(2)} &= 15.111L^2 + 31.6617L + 2.38332 + i(23.7365L + 28.0745), \\
D_{8L}^{(2)} &= -1.7778L^2 - 4.0386L - 1.7170 - i(2.7925L + 4.4215), \\
D_{8H}^{(2)} &= -1.7778L^2 - 4.0386L + 0.8829 - i2.7925L.
\end{aligned} \tag{89}$$

7.2 The coefficients $\Delta_1 C^{B1(0)}$, $\Delta_7 C^{B1(1)}$ and $j_\perp^{(1)}$

Here we list the coefficients needed for the numerical analysis of spectator scattering which are not written in main text. The lowest order expression for $\Delta_1 C^{B1}$ is [34]

$$\Delta_1 C^{B1(0)}(u) = \frac{E_\gamma}{4\pi^2}\frac{2e}{3} f\left(\frac{m_c^2}{\bar u m_b^2}\right), \tag{90}$$

where

$$f(x) = \theta\left(\frac{1}{4}-x\right)\left[1+4x\left(\mathrm{arctanh}(\sqrt{1-4x})-i\frac{\pi}{2}\right)^2\right] + \theta\left(x-\frac{1}{4}\right)\left[1-4x\left(\arctan^2\frac{1}{\sqrt{4x-1}}\right)\right]. \quad (91)$$

For Q_7 the tree-level coefficient was given in (35). The one-loop correction is [39, 42]

$$\begin{aligned}\frac{\Delta_7 C^{B1(1)}}{\Delta_7 C^{B1(0)}} &= \frac{C_F\alpha_s}{4\pi}\frac{1}{2}\Bigg\{-4\ln^2\frac{\mu}{m_b}-2\ln\frac{\mu}{m_b}-4\ln\frac{\mu_{\rm QCD}}{m_b}-\frac{\pi^2}{6}-\frac{4}{u}\ln\bar u-2 \\ &+\frac{4\bar u}{u}\left[\left(-2\ln\frac{\mu}{m_b}-1\right)\ln\bar u+\ln^2\bar u+\mathrm{Li}_2(u)\right]\Bigg\} \\ &+\frac{1}{2}\left(C_F-\frac{C_A}{2}\right)\frac{\alpha_s}{4\pi}\Bigg\{-\frac{4\bar u}{u}\left[\left(-2\ln\frac{\mu}{m_b}-1\right)\ln\bar u+\ln^2\bar u+\mathrm{Li}_2(u)\right] \\ &-\frac{4(2-u)}{\bar u}\left[\left(-2\ln\frac{\mu}{m_b}-1\right)\ln u+\ln^2 u+\mathrm{Li}_2(\bar u)\right] \\ &+\frac{4}{\bar u u}\mathrm{Li}_2(\bar u)+\frac{4}{u}\left[\mathrm{Li}_2(u)-\frac{\pi^2}{6}\right]+4\ln\bar u-4\ln u-4\Bigg\}. \end{aligned} \quad (92)$$

The one-loop correction to the jet function can be obtained from, e.g., eq. (79) of [40] after appropriate replacements. Calling the one-loop correction defined in eq. (79) of [40] $j_\perp^{\rm BY}$ after the authors of that paper, we have

$$j_\perp^{(1)}(\tau,u,\omega) = -\frac{4\pi C_F\alpha_s}{N_c}\frac{1}{m_b\omega\bar u}\delta(\tau-u)\left[\frac{\alpha_s}{4\pi}\,j_\perp^{\rm BY}(\bar\tau;u,\omega)\right]. \quad (93)$$

7.3 RG functions

Here we summarize the perturbative solutions to the RG exponents in (30, 71). We define the expansion coefficients of the anomalous dimensions and the β-function as

$$\begin{aligned}\Gamma_{\rm cusp}(\alpha_s) &= \Gamma_0\frac{\alpha_s}{4\pi}+\Gamma_1\left(\frac{\alpha_s}{4\pi}\right)^2+\Gamma_2\left(\frac{\alpha_s}{4\pi}\right)^3+\dots, \\ \beta(\alpha_s) &= -2\alpha_s\left[\beta_0\frac{\alpha_s}{4\pi}+\beta_1\left(\frac{\alpha_s}{4\pi}\right)^2+\beta_2\left(\frac{\alpha_s}{4\pi}\right)^3+\dots\right], \end{aligned} \quad (94)$$

and similarly for the anomalous dimension γ_J. In terms of these quantities, the function a (and a_J with obvious replacements) is given by

$$a(\nu,\mu) = -\frac{\Gamma_0}{2\beta_0}\left[\ln\frac{\alpha_s(\mu)}{\alpha_s(\nu)}+\left(\frac{\Gamma_1}{\Gamma_0}-\frac{\beta_1}{\beta_0}\right)\frac{\alpha_s(\mu)-\alpha_s(\nu)}{4\pi}\right]. \quad (95)$$

The result for the Sudakov factor S to this same order is

$$\begin{aligned}S(\nu,\mu) &= \frac{\Gamma_0}{4\beta_0^2}\Bigg\{\frac{4\pi}{\alpha_s(\nu)}\left(1-\frac{1}{r}-\ln r\right)+\left(\frac{\Gamma_1}{\Gamma_0}-\frac{\beta_1}{\beta_0}\right)(1-r+\ln r)+\frac{\beta_1}{2\beta_0}\ln^2 r \\ &+\frac{\alpha_s(\nu)}{4\pi}\Bigg[\left(\frac{\beta_1\Gamma_1}{\beta_0\Gamma_0}-\frac{\beta_2}{\beta_0}\right)(1-r+r\ln r)+\left(\frac{\beta_1^2}{\beta_0^2}-\frac{\beta_2}{\beta_0}\right)(1-r)\ln r \\ &-\left(\frac{\beta_1^2}{\beta_0^2}-\frac{\beta_2}{\beta_0}-\frac{\beta_1\Gamma_1}{\beta_0\Gamma_0}+\frac{\Gamma_2}{\Gamma_0}\right)\frac{(1-r)^2}{2}\Bigg]\Bigg\}, \end{aligned} \quad (96)$$

where $r = \alpha_s(\mu)/\alpha_s(\nu)$. The cusp anomalous dimension to three loops is

$$\begin{aligned}
\Gamma_0 &= 4C_F\,, \\
\Gamma_1 &= 4C_F\left[\left(\frac{67}{9}-\frac{\pi^2}{3}\right)C_A - \frac{20}{9}T_F n_f\right], \\
\Gamma_2 &= 4C_F\Bigg[C_A^2\left(\frac{245}{6}-\frac{134\pi^2}{27}+\frac{11\pi^4}{45}+\frac{22}{3}\zeta_3\right)+C_A T_F n_f\left(-\frac{418}{27}+\frac{40\pi^2}{27}-\frac{56}{3}\zeta_3\right) \\
&\quad + C_F T_F n_f\left(-\frac{55}{3}+16\zeta_3\right)-\frac{16}{27}T_F^2 n_f^2\Bigg],
\end{aligned} \tag{97}$$

and the QCD β function is

$$\begin{aligned}
\beta_0 &= \frac{11}{3}C_A - \frac{4}{3}T_F n_f\,, \\
\beta_1 &= \frac{34}{3}C_A^2 - \frac{20}{3}C_A T_F n_f - 4C_F T_F n_f\,, \\
\beta_2 &= \frac{2857}{54}C_A^3 + \left(2C_F^2 - \frac{205}{9}C_F C_A - \frac{1415}{27}C_A^2\right)T_F n_f + \left(\frac{44}{9}C_F + \frac{158}{27}C_A\right)T_F^2 n_f^2.
\end{aligned} \tag{98}$$

7.4 Separating scales in the $\Delta_i C^A$ coefficients

Here we list the NNLO coefficients $\Delta_i C^A$ in the case where we distinguish $L_{\rm QCD}$ from L. This is achieved by solving the RG equation (25) perturbatively, given the form (22) for the anomalous dimension γ^A. This has been done in [74] and we can use those results after making appropriate replacements. We find

$$\begin{aligned}
\Delta_7 C^{A(2)} &= C_F^2\big[2L^4+10L^3+4L^2L_{\rm QCD}+26.1449L^2+10LL_{\rm QCD}+2L_{\rm QCD}^2 \\
&\quad +23.5022L+32.6449L_{\rm QCD}+7.8159\big] \\
&\quad +C_F C_A\big[-4.8889L^3-26.6425L^2-14.6667LL_{\rm QCD}+7.33333L_{\rm QCD}^2 \\
&\quad -63.7859L-28.5556L_{\rm QCD}-83.8866\big] \\
&\quad +C_F n_l\big[0.8889L^3+5.5556L^2+2.6667LL_{\rm QCD}-1.3333L_{\rm QCD}^2 \\
&\quad +17.0161L+2.8889L_{\rm QCD}+23.8254\big] \\
&\quad +C_F n_h\left(-1.3333L_{\rm QCD}^2+2.8889L_{\rm QCD}-0.810288\right),
\end{aligned} \tag{99}$$

$$\begin{aligned}
\Delta_8 C^{A(2)} &= -C_F^2\big[5.3333L^2L_{\rm QCD}+2.9468L^2+13.333LL_{\rm QCD}+16L_{\rm QCD}^2 \\
&\quad +7.3671L+43.5941L_{\rm QCD}+1.8875 \\
&\quad +i(4.1888L^2+10.4720L+20.9440L_{\rm QCD}+29.8299)\big] \\
&\quad +C_F C_A\big[19.5556LL_{\rm QCD}-4.4444L_{\rm QCD}^2+10.8051L+20.8566L_{\rm QCD}+2.3833 \\
&\quad +i(15.3589L+8.3776L_{\rm QCD}+28.0745)\big] \\
&\quad -C_F n_l\big[3.5556LL_{\rm QCD}-1.7778L_{\rm QCD}^2+1.9646L+2.0741L_{\rm QCD}+1.7170 \\
&\quad +i(2.7925L+4.4215)\big] \\
&\quad +C_F n_h\big[1.7778L_{\rm QCD}^2-2.0741L_{\rm QCD}+0.8829\big],
\end{aligned} \tag{100}$$

$$\Delta_1 C^{A(2)} = -\frac{3\beta_0}{2}\frac{m_b}{\overline{m}_b}C_F\left[2.4691 L_{\rm QCD}^2 + l^{(2)}(z) L_{\rm QCD} + r^{(2)}(z)\right] - 2\beta_0 L_{\rm QCD}\Delta_1 C^{A(1)} + 2\beta_0 L \Delta_1 C^{A(1)}\,. \quad (101)$$

References

[1] T. E. Coan *et al.* [CLEO Collaboration], Phys. Rev. Lett. **84**, 5283 (2000) [arXiv:hep-ex/9912057].

[2] B. Aubert *et al.* [BABAR Collaboration], Phys. Rev. D **70**: 112006 (2004) [arXiv:hep-ex/0407003].

[3] M. Nakao *et al.* [BELLE Collaboration], Phys. Rev. D **69**: 112001 (2004) [arXiv:hep-ex/0402042].

[4] K. Abe *et al.* [BELLE Collaboration], Phys. Rev. Lett. **96**: 221601 (2006) [arXiv:hep-ex/0506079].

[5] B. Aubert *et al.* [BABAR Collaboration], SLAC-PUB-12025, BABAR-CONF-06-034 [arXiv:hep-ex/0607099].

[6] M. Nakao [BELLE Collaboration], in Proceedings of the XXIII International Symposium on Lepton and Photon Interactions at High Energy (Lepton-Photon-2007), August 13 -18, 2007, Daego, Korea.

[7] The Heavy Flavor Averaging Group (HFAG) (April 2007 Update), http://www.slac.stanford.edu/xorg/hfag/ and arXiv:0704.3575 [hep-ex].

[8] A. Abulencia *et al.* [CDF Collaboration], Phys. Rev. Lett. **97**: 242003 (2006) [arXiv:hep-ex/0609040].

[9] G. Buchalla, A. J. Buras and M. E. Lautenbacher, Rev. Mod. Phys. **68**, 1125 (1996) [arXiv:hep-ph/9512380].

[10] M. Beneke, G. Buchalla, M. Neubert and C. T. Sachrajda, Nucl. Phys. B **591**, 313 (2000) [arXiv:hep-ph/0006124].

[11] T. Hurth, Rev. Mod. Phys. **75**, 1159 (2003) [arXiv:hep-ph/0212304].

[12] C. Bobeth, M. Misiak and J. Urban, Nucl. Phys. B **574**, 291 (2000) [arXiv:hep-ph/9910220].

[13] M. Misiak and M. Steinhauser, Nucl. Phys. B **683**, 277 (2004) [arXiv:hep-ph/0401041].

[14] M. Gorbahn and U. Haisch, Nucl. Phys. B **713**, 291 (2005) [arXiv:hep-ph/0411071].

[15] M. Gorbahn, U. Haisch and M. Misiak, Phys. Rev. Lett. **95**, 102004 (2005) [arXiv:hep-ph/0504194].

[16] M. Czakon, U. Haisch and M. Misiak, JHEP **0703**, 008 (2007) [arXiv:hep-ph/0612329].

[17] A. Ali and A. Y. Parkhomenko, Eur. Phys. J. C **23**, 89 (2002) [arXiv:hep-ph/0105302].

[18] A. Ali, E. Lunghi and A. Y. Parkhomenko, Phys. Lett. B **595**, 323 (2004) [arXiv:hep-ph/0405075].

[19] M. Beneke, T. Feldmann and D. Seidel, Nucl. Phys. B **612**, 25 (2001) [arXiv:hep-ph/0106067].

[20] A. L. Kagan and M. Neubert, Phys. Lett. B **539**, 227 (2002) [arXiv:hep-ph/0110078].

[21] S. W. Bosch and G. Buchalla, Nucl. Phys. B **621**, 459 (2002) [arXiv:hep-ph/0106081].

[22] S. W. Bosch and G. Buchalla, JHEP **0501**, 035 (2005) [arXiv:hep-ph/0408231].

[23] M. Beneke, T. Feldmann and D. Seidel, Eur. Phys. J. C **41**, 173 (2005) [arXiv:hep-ph/0412400].

[24] A. Ali and A. Parkhomenko, DESY 06-187 (2006) [arXiv:hep-ph/0610149].

[25] P. Ball, G. W. Jones and R. Zwicky, Phys. Rev. D **75**, 054004 (2007) [arXiv:hep-ph/0612081].

[26] Y. Y. Keum, M. Matsumori and A. I. Sanda, Phys. Rev. D **72**, 014013 (2005) [arXiv:hep-ph/0406055].

[27] C. D. Lü, M. Matsumori, A. I. Sanda and M. Z. Yang, Phys. Rev. D **72**, 094005 (2005) [Erratum-ibid. D **73**, 039902 (2006)] [arXiv:hep-ph/0508300].

[28] C. W. Bauer, S. Fleming and M. E. Luke, Phys. Rev. D **63**, 014006 (2001) [arXiv:hep-ph/0005275].

[29] C. W. Bauer, S. Fleming, D. Pirjol and I. W. Stewart, Phys. Rev. D **63**, 114020 (2001) [arXiv:hep-ph/0011336].

[30] C. W. Bauer, D. Pirjol and I. W. Stewart, Phys. Rev. D **65**, 054022 (2002) [arXiv:hep-ph/0109045].

[31] M. Beneke, A. P. Chapovsky, M. Diehl and T. Feldmann, Nucl. Phys. B **643**, 431 (2002) [arXiv:hep-ph/0206152].

[32] J. g. Chay and C. Kim, Phys. Rev. D **68**, 034013 (2003) [arXiv:hep-ph/0305033].

[33] B. Grinstein, Y. Grossman, Z. Ligeti and D. Pirjol, Phys. Rev. D **71**, 011504 (2005) [arXiv:hep-ph/0412019].

[34] T. Becher, R. J. Hill and M. Neubert, Phys. Rev. D **72**, 094017 (2005) [arXiv:hep-ph/0503263].

[35] M. Beneke and T. Feldmann, Nucl. Phys. B **592**, 3 (2001) [arXiv:hep-ph/0008255].

[36] C. W. Bauer, D. Pirjol and I. W. Stewart, Phys. Rev. D **67** (2003) 071502 [arXiv:hep-ph/0211069].

[37] M. Beneke and T. Feldmann, Nucl. Phys. B **685**, 249 (2004) [arXiv:hep-ph/0311335].

[38] B. O. Lange and M. Neubert, Nucl. Phys. B **690**, 249 (2004) [Erratum-ibid. B **723**, 201 (2005)] [arXiv:hep-ph/0311345].

[39] M. Beneke, Y. Kiyo and D. s. Yang, Nucl. Phys. B **692**, 232 (2004) [arXiv:hep-ph/0402241].

[40] M. Beneke and D. Yang, Nucl. Phys. B **736**, 34 (2006) [arXiv:hep-ph/0508250].

[41] R. J. Hill, T. Becher, S. J. Lee and M. Neubert, JHEP **0407**, 081 (2004) [arXiv:hep-ph/0404217].

[42] T. Becher and R. J. Hill, JHEP **0410**, 055 (2004) [arXiv:hep-ph/0408344].

[43] I. Blokland, A. Czarnecki, M. Misiak, M. Slusarczyk and F. Tkachov, Phys. Rev. D **72**, 033014 (2005) [arXiv:hep-ph/0506055].

[44] H. M. Asatrian, A. Hovhannisyan, V. Poghosyan, T. Ewerth, C. Greub and T. Hurth, Nucl. Phys. B **749**, 325 (2006) [arXiv:hep-ph/0605009].

[45] H.M. Asatrian, T. Ewerth, A. Ferroglia, P. Gambino, C. Greub and G. Ossola, in preparation.

[46] C. Greub, T. Hurth and D. Wyler, Phys. Rev. D **54**, 3350 (1996) [arXiv:hep-ph/9603404].

[47] A. J. Buras, A. Czarnecki, M. Misiak and J. Urban, Nucl. Phys. B **611**, 488 (2001) [arXiv:hep-ph/0105160].

[48] A. J. Buras, A. Czarnecki, M. Misiak and J. Urban, Nucl. Phys. B **631**, 219 (2002) [arXiv:hep-ph/0203135].

[49] K. Bieri, C. Greub and M. Steinhauser, Phys. Rev. D **67**, 114019 (2003) [arXiv:hep-ph/0302051].

[50] R. Boughezal, M. Czakon and T. Schutzmeier, JHEP **0709**, 072 (2007) [arXiv:0707.3090 [hep-ph]].

[51] M. Beneke and V. M. Braun, Phys. Lett. B **348** (1995) 513 [arXiv:hep-ph/9411229].

[52] M. Misiak and M. Steinhauser, Nucl. Phys. B **764**, 62 (2007) [arXiv:hep-ph/0609241].

[53] M. Misiak *et al.*, Phys. Rev. Lett. **98**, 022002 (2007) [arXiv:hep-ph/0609232].

[54] M. Beneke and S. Jäger, Nucl. Phys. B **751**, 160 (2006) [arXiv:hep-ph/0512351].

[55] M. Beneke and S. Jäger, Nucl. Phys. B **768**, 51 (2007) [arXiv:hep-ph/0610322]. Phys. Rev. Lett. **98**: 022002 (2007) [arXiv:hep-ph/0609232].

[56] M. Beneke and V. A. Smirnov, Nucl. Phys. B **522**, 321 (1998) [arXiv:hep-ph/9711391].

[57] G. G. Kirilin, arXiv:hep-ph/0508235.

[58] N. Kivel, JHEP **0705** (2007) 019 [arXiv:hep-ph/0608291].

[59] A. V. Manohar and I. W. Stewart, MIT-CTP-3726, UCSD-PTH-06-04 (2006) [arXiv:hep-ph/0605001].

[60] M. Steinhauser, Phys. Rept. **364**, 247 (2002) [arXiv:hep-ph/0201075].

[61] I. A. Korchemskaya and G. P. Korchemsky, Phys. Lett. B **287**, 169 (1992).

[62] S. Moch, J. A. M. Vermaseren and A. Vogt, Nucl. Phys. B **688**, 101 (2004) [hep-ph/0403192].

[63] M. Neubert, Eur. Phys. J. C **40**, 165 (2005) [arXiv:hep-ph/0408179].

[64] T. Becher and M. Neubert, Phys. Rev. Lett. **98**, 022003 (2007) [arXiv:hep-ph/0610067].

[65] T. Becher and M. Neubert, Phys. Lett. B **633**, 739 (2006) [arXiv:hep-ph/0512208].

[66] T. Becher and M. Neubert, Phys. Lett. B **637**, 251 (2006) [arXiv:hep-ph/0603140].

[67] S. Descotes-Genon and C. T. Sachrajda, Nucl. Phys. B **693**, 103 (2004) [arXiv:hep-ph/0403277].

[68] G. P. Lepage and S. J. Brodsky, Phys. Rev. D **22**, 2157 (1980).

[69] A. V. Efremov and A. V. Radyushkin, Phys. Lett. B **94**, 245 (1980).

[70] B. O. Lange and M. Neubert, Phys. Rev. Lett. **91**, 102001 (2003) [arXiv:hep-ph/0303082].

[71] S. W. Bosch, R. J. Hill, B. O. Lange and M. Neubert, Phys. Rev. D **67**, 094014 (2003) [arXiv:hep-ph/0301123].

[72] V. M. Braun, D. Y. Ivanov and G. P. Korchemsky, Phys. Rev. D **69**, 034014 (2004) [arXiv:hep-ph/0309330].

[73] X. D. Ji and M. J. Musolf, Phys. Lett. B **257**, 409 (1991).

[74] M. Neubert, Phys. Rev. D **72**, 074025 (2005) [arXiv:hep-ph/0506245].